Research Article

Fate and effects of graphene oxide alone and with sorbed benzo(a)pyrene in mussels *Mytilus galloprovincialis*

Nagore González-Soto [a], Nagore Blasco [a], Mireia Irazola [b], Eider Bilbao [a], Lúcia Guilhermino [c], Miren P. Cajaraville [a,*]

[a] CBET Research Group, Dept. Zoology and Animal Cell Biology, Science and Technology Faculty and Plentzia Marine Station, University of the Basque Country (UPV/EHU), Basque Country, Spain
[b] Dept. Analytical Chemistry and Plentzia Marine Station, University of the Basque Country (UPV/EHU), Basque Country, Spain
[c] Ecotoxicology Research Group, ICBAS, Institute of Biomedical Sciences of Abel Salazar and Research Group of Ecotoxicology, Stress Ecology and Environmental Health (ECOTOX), CIIMAR, Interdisciplinary Centre of Marine and Environmental Research, University of Porto, Portugal

HIGHLIGHTS

- GO was found in digestive tract lumen and feces of mussels exposed to GO or GO+BaP.
- BaP bioaccumulated in mussels exposed to GO+BaP and especially to BaP.
- An environmentally relevant concentration of GO was genotoxic to mussel hemocytes.
- Inflammation in digestive gland/gonad and oocyte atresia found in exposed mussels.
- Effects of carried BaP and enhanced toxicity of GO+BaP vs GO or BaP were identified.

GRAPHICAL ABSTRACT
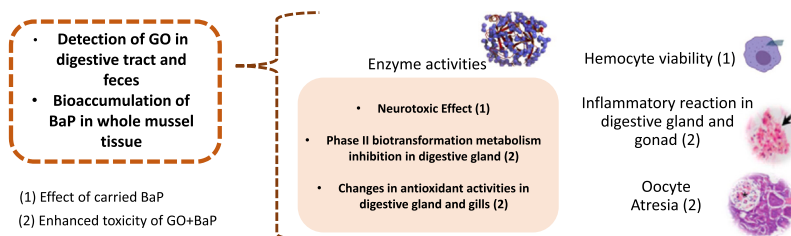
ARTICLE INFO

Editor: Karina S. B. Miglioranza

ABSTRACT

Graphene oxide (GO) has gained a great scientific and economic interest due to its unique properties. As incorporation of GO in consumer products is rising, it is expected that GO will end up in oceans. Due to its high surface to volume ratio, GO can adsorb persistent organic pollutants (POPs), such as benzo(a)pyrene (BaP), and act as carrier of POPs, increasing their bioavailability to marine organisms. Thus, uptake and effects of GO in marine biota represent a major concern. This work aimed to assess the potential hazards of GO, alone or with sorbed BaP (GO+BaP), and BaP alone in marine mussels after 7 days of exposure. GO was detected through Raman spectroscopy in the lumen of the digestive tract and in feces of mussels exposed to GO and GO+BaP while BaP was bioaccumulated in mussels exposed to GO+BaP, but especially in those exposed to BaP. Overall, GO acted as a carrier of BaP to mussels but GO appeared to protect mussels towards BaP accumulation. Some effects

observed in mussels exposed to GO+BaP were due to BaP carried onto GO nanoplatelets. Enhanced toxicity of GO+BaP with respect to GO and/or BaP or to controls were identified for other biological responses, demonstrating the complexity of interactions between GO and BaP.

1. Introduction

Nanomaterials (NMs) are commonly defined as a diverse class of materials with at least one dimension at the nanoscale (<100 nm) [1]. In 2011, the European Commission defined a nanomaterial as: "*a natural, incidental or manufactured material containing particles, in an unbound state or as an aggregate or as an agglomerate and where, for 50% or more of the particles in the number size distribution, one or more external dimensions is in the size range 1–100 nm. In specific cases and where warranted by concerns for the environment, health, safety or competitiveness the number size distribution threshold of 50% may be replaced by a threshold between 1% and 50%* [2]. Among NMs, carbon-based NMs have attracted great scientific and technological attention due to the physico-chemical properties of their nanometric structures. Carbon-based NMs include among others, fullerenes, carbon nanotubes, carbon black or graphene; but among all of them, graphene stands out for the unique properties that make it the thinnest, strongest and lightest known material [3].

Graphene family nanomaterials (GFNs) are used in a wide range of applications including electronic devices, a new generation of batteries, sensors [4], biomedical applications [5], anticorrosion coatings [6,7], agricultural procedures [8] or environmental applications such as waste water treatments [4], water desalination [9] and pollutants removal [4, 10]. There are more than 26,000 graphene related patents [11] and more than 100 graphene based products [12]. In fact, the production of GFNs is higher in comparison to the rest of NMs [13] and it is expected to continue growing as the expensive and low efficient methods used nowadays for graphene production are improved. Therefore, graphene production is expected to reach 3800 tones, with a worth of 300 millions by 2027 [14].

Graphene oxide (GO) is a precursor in graphene synthesis and one of the most studied graphene derivates [15] whose reactivity and capacity for chemical functionalization [12] are important characteristics related to the presence of functional oxygen groups both on the surface (hydroxyl and epoxy groups) and in the edges (carboxyl groups) of the sheet [16]. Due to the general interest on GO and its increased production in the last years, GO is being released into the environment during its life cycle [17] both through direct release (e.g., sewage effluents, river influx) or indirectly (e.g., aerial deposition, dumping and run off) [18]. Therefore, GO will definitely reach coastal and marine ecosystems [12] and probably will interact with different components of the natural system, which may alter behaviour, transport, fate and toxicity of GO [19]. Transport and fate of GFNs are governed mainly by the stability of suspensions, which may be altered by environmental factors such as salinity, organic matter concentration, oxidation status and bioturbation. In aquatic environments, GO can disperse and form relatively stable suspensions that endure in the water column [18,20]. Such behavior may facilitate the uptake of GO by a large number of organisms through different routes such as ingestion or respiration, as it has been described for other NMs [21]. In addition, the high persistence of GO can result in their bioaccumulation and biomagnification in food webs [4, 22], increasing their potential impact in marine ecosystems, even if the GO concentrations released into the environment are relatively low [23]. Therefore, levels of GO in surface waters should be a primary concern [24]. However, the environmental concentrations of GO are still largely unknown [12]. The presence of GO was already detected in the biomass from wastewater treatment plants [25]. Recent studies consider that the predicted environmental concentration of GO could be similar to that described for other NMs such as multi-walled carbon nanotubes, which is in the range 0.001–1000 µg/L for aquatic environments [26].

Toxicity of NMs is strongly related to their size, shape, surface properties or chemical composition, which are key characteristics for risk assessment [1,27]. Overall, at cellular level, GFNs have been reported to decrease integrity of the cell's plasma membrane, possibly as a consequence of entry of nanosheets into cells by direct penetration or endocytosis [18]. Sheets can also disrupt the plasma membrane due to induced invaginations or perforations [28,29], or even by the destructive extraction of lipids [30]. Disruption of the plasma membrane and internalization of GFNs can provoke the formation of reactive oxygen species (ROS) and lead to oxidative stress [29], which is considered one of the main underlying mechanisms of toxicity of NMs [27]. Oxidative damage caused by the increased intracellular production of ROS can lead to mitochondrial and lysosomal dysfunction and finally to a decrease in the viability of hemocyte cells of marine mussels [29]. In addition, oxidative stress and/or physical cell damage can also cause DNA damage resulting in the fragmentation and destruction of nucleic acids [31]. These alterations at the cellular level may lead to effects at higher biological levels, such as reduction of metabolic activity [4,32], histopathological lesions [33,34], alterations in behavior and locomotor functions [35] and adverse impact on the reproduction capacity, growth and survival [36].

In aquatic environments, generally NMs do not appear alone, but are found within complex mixtures of chemical contaminants originated both from natural and anthropogenic sources. Several studies have demonstrated that GFNs show a great adsorption capacity for persistent organic pollutants (POPs) such as polycyclic aromatic hydrocarbons (PAHs), mainly due to their large surface area and hydrophobicity [37–40]. This adsorption produces accumulation of organic pollutants on the surface of the NM, which may increase their uptake by aquatic organisms [41] and their potential adverse effects [39], a phenomenon known as Trojan horse effect.

Originally, Limbach et al. [42] introduced the Trojan horse concept to refer to the extended toxicity caused by metal nanoparticles in comparison to their soluble forms, due to the continuous release of metal ions in and out of cells. Later, carrier or Trojan horse effect was introduced to designate the increased uptake and accumulation of environmental pollutants facilitated by NMs [43,44]. Thus, the Trojan horse effect is generally defined as the possible threat of NMs due to their ability to adsorb and carry adsorbed compounds to organisms, a phenomenon known to occur for many NMs and several metal or organic pollutants [45–48]. Most works are based on co-exposure of NMs and environmental pollutants and the toxicity of the mixture is usually compared to that of the dissolved pollutant and not to that of the NM alone [46,48] which could lead to an underestimation of the contribution of the NM to the toxicity of the mixture [46]. Different reviews consider that a Trojan horse effect occurs when the exposure to the mixture causes a significantly higher toxicological effect than the exposure to the compounds separately [45–50].

Among PAHs, benzo(a)pyrene (BaP) is a priority pollutant [51,52], commonly used in ecotoxicology studies and known to cause effects at different levels of biological organization [53]. BaP is a genotoxic and carcinogenic agent capable of producing tissue and DNA damage [54, 55], oxidative stress [56], peroxisome proliferation [57], lysosomal dysfunction [58], endocrine disruption [59], among other effects in marine organisms, including bivalves. In addition, BaP can interact with emerging pollutants of high concern, such as microplastics and NMs, in marine mussels resulting in toxicological interactions [55,60]. Among target organisms, mussels (*Mytilus sp.*), are considered model organisms for the evaluation of pollutants including micro and nanoscale particulate materials, due to their highly developed mechanisms for cellular internalization of particles through endocytosis and phagocytosis, for
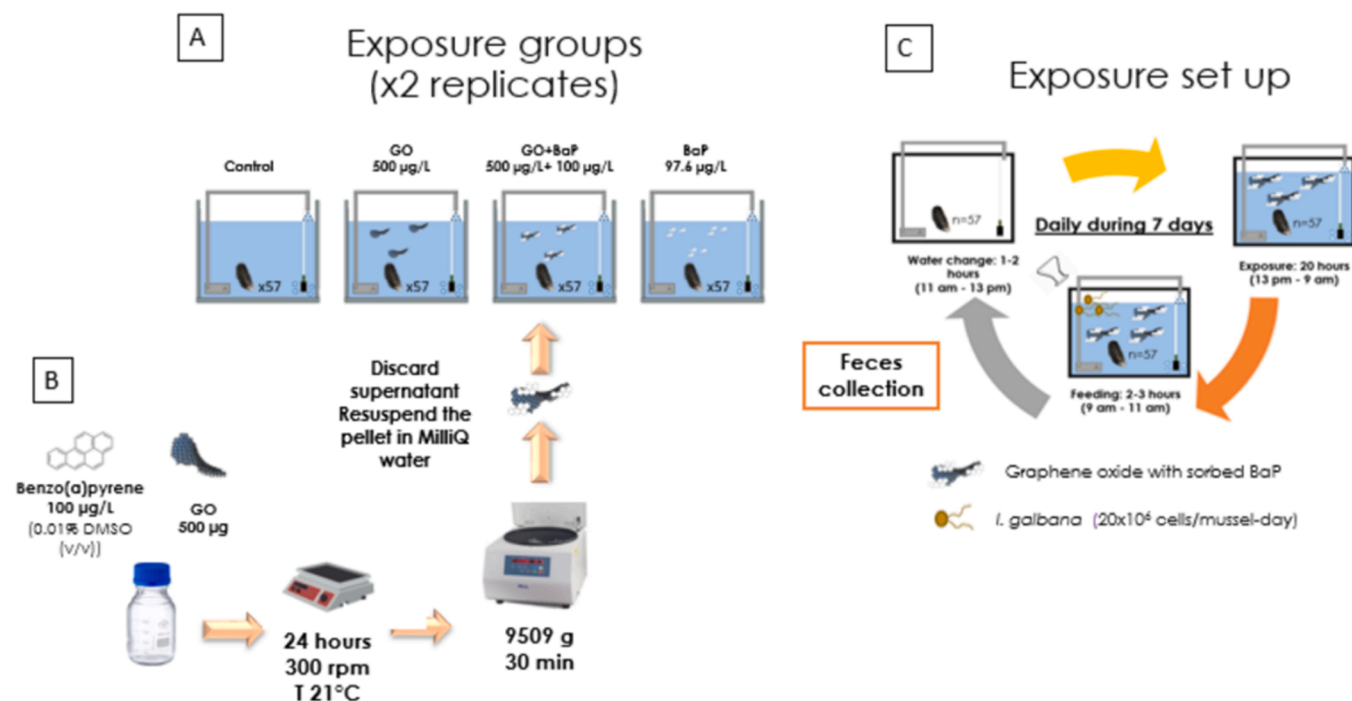
Fig. 1. Summary of the experimental design. A: Exposure groups, B: preparation of graphene oxide (GO) with adsorbed benzo(a)pyrene (BaP) and C: exposure set up for the GO+BaP group as an example.

physiological functions such as intracellular digestion and cellular immunity [27,61,62].

To improve the basis for the risk assessment of GFNs to the marine environment, it is very important to study the toxicity of GFNs, alone and combined with POPs in marine organisms, such as mussels. Therefore, the aim of this work was to investigate the fate and effects of GO, alone or with sorbed BaP, in adult marine mussels (*M. galloprovincialis*) using Raman spectroscopy and a battery of biological responses, respectively. Overall, this work contributes to understand the Trojan horse effect of GFNs towards BaP in mussels.

2. Materials and methods

2.1. Obtention of GO and preparation of GO with sorbed BaP

Commercial nanoplatelets of graphene oxide (GO) were purchased from Graphenea (San Sebastian, Spain) as stable suspensions. According to the supplier, the concentration of GO in the dispersion was 10 mg/mL. This was experimentally confirmed by measuring GO in aqueous dispersions with a UV–vis spectrophotometer (UV-2550, Shimadzu) at 660 nm, where graphene follows the Lambert-Beer law. For that aim, a calibration curve (Fig. S1) was prepared from dispersions with known GO concentrations. The concentration of GO experimentally determined was 9.91 mg/mL.

According to the manufacturer's information, nanoplatelets showed lateral dimensions ranging from 500 nm to few microns and thickness was < 2 nm. Oxygen content was about 40% wt. Characterization of the same batch of GO by transmission electron microscopy and atomic force microscopy was reported previously by Martínez-Álvarez et al. [63].

The protocol to prepare GO with sorbed benzo(a)pyrene (BaP) was based on previous work (Martínez-Álvarez et al. [63]). Briefly, after preparing the BaP solution of 100 μg/L containing 0.01% dimethyl sulfoxide (DMSO, purity 99% Sigma, St. Louis, Missouri) in a glass bottle, GO was added in a 0.5 mg:10 mL GO/BaP proportion (weight/-volume). Sorption process was allowed by shaking samples in an orbital shaker (300 rpm) for 24 h in the dark at 21 ± 1 °C. After 24 h, samples were centrifuged in an Allegra X30R centrifuge (9509 g, 30 min).

Supernatant was discarded and the pellet was re-suspended in 50 mL of MilliQ water. Samples were vortexed before dosing into tanks. Samples containing GO alone were processed in the same way, but using only MilliQ water.

For sorption experiments [63], samples were prepared in the same way described above. After centrifugation, absence of GO in supernatants was assessed by spectrophotometry at 230 nm. Then, BaP was quantified in supernatants by gas chromatography/mass spectrometry after solid phase micro extraction. Based on the BaP concentration measured in the aqueous phase, the amount of BaP sorbed to GO was indirectly calculated. This process was done in triplicate and vials containing BaP solutions without GO were processed in parallel to monitor potential BaP loss due to evaporation, degradation, sorption onto the vial walls or other factors during the experimental procedure. According to Martínez-Álvarez et al. [63] the proportion of BaP sorbed onto GO was 96.7% ± 0.5%.

2.2. Sampling and acclimation of mussels

Roughly 460 mussels *Mytilus galloprovincialis* (3.5–4.5 cm shell length) were collected in February 2019 in Mundaka, Basque Country (43°24′04.9″N, 2°41′41.6″W). Mussels were maintained in aquaria facilities at the Plentzia Marine Station (PiE) of the University of the Basque Country (UPV/EHU), for acclimation during 21 days. Acclimation was carried out in a 300 L polypropylene tank with a recirculating seawater system. Marine water was collected with a pump at 10 m depth in the mouth of the Butroi estuary (43°24′21″N, 2°56′47″W) and filtered (particles ≤ 3 μm) before reaching the marine station. Mussels were not fed for two days and then they were fed once a day with the *Isochrysis galbana* microalgae (2×10^7 cells/mussel-day) for 19 days. *I. galbana* (T-Iso clone) cultures were obtained from the Animal Physiology Laboratory at UPV/EHU. During acclimation, light regime was 12 L/12D and room temperature was kept at 18 °C. Water parameters were checked daily with a multichannel probe. The variation of water parameters during the acclimation period was (mean ± standard deviation): salinity of 32.40 ± 0.27, pH of 7.25 ± 0.35 and temperature of 16.02 ± 0.08 °C. The dissolved O_2 was always above 80%.

2.3. Mussel exposure

In order to keep a homogeneous suspension of GO, without aggregation or precipitation, a water recirculation system consisting of two water pumps was installed in the aquaria. Before mussel exposure, tanks were exposed for 24 h to GO at the same concentration tested in order to saturate the system.

After 21 days of acclimation, mussels were exposed for 7 days to graphene oxide (GO), graphene oxide with sorbed BaP (GO+BaP) or BaP alone in two 20 L replicate tanks per treatment (GO R1 and GO R2, GO+BaP R1 and GO+BaP R2, BaP R1 and BaP R2) with 57 mussels each (Fig. 1). Two control tanks, also with 57 mussels each, were run in parallel (Control R1, Control R2). Mussel samples were taken after 7 days of exposure. An exposure concentration of 500 μg/L GO was selected, based on environmentally relevant concentrations for multi-walled carbon nanotubes, which range from 1 μg/L to 1 mg/L [12]. For the GO+BaP exposure groups, the nominal concentration of BaP incubated with GO was 100 μg/L. Finally, for the BaP exposure groups, 96.7 μg/L BaP was used as the equivalent BaP concentration sorbed in GO+BaP preparations [63].

During the experiment, water was changed daily. Throughout exposure, mussels were fed once a day with *I. galbana* (2×10^7 cells /mussel-day) two hours before changing water. While water of tanks was changed, 5 mussels per tank were selected randomly and placed in individual glass containers with clean water to collect feces (Fig. 1). The light regime and room temperature were kept at 12 L/12D and 18 °C, respectively. Water parameters were checked daily with a multichannel probe: salinity (32.93 ± 0.06 PSU), dissolved O_2 (>77%), pH (7.48 $\pm$ 0.23) and temperature (16.62 ± 0.25 °C).

2.4. Bioaccumulation of BaP

The presence of BaP in seawater was checked by gas chromatography–mass spectrometry (GC–MS) analysis in water collected after 20 h of exposure in all the tanks according to the protocol described in Katsumiti et al. [64]. Briefly, twister stir bars (20 mm length and 0.5 mm film thick, Gerstel GmbH & Co. KG, Mülheim an der Ruhr, Germany) were employed for extraction of BaP from the marine water. Twister bars were introduced in samples (~20 mL) during 195 min. Then, twister bars were cleaned with Milli-Q water and dried with paper tissue. BaP was desorbed from the twister bars using a commercial thermal desorption TDS-2 unit connected to a CIS-4 injector (Gerstel GmbH & Co. KG, Mülheiman der Ruhr, Germany). The desorption unit was then connected to an Agilent 6890 gas chromatograph coupled with an Agilent 5975 mass spectrometer system (Agilent Technologies, Palo Alto, USA) for BaP determination.

Mussels for chemical analysis (14–18 mussels per tank) were stored at − 40 °C and analyzed at IPROMA (Castellon, Spain) to determine bioaccumulation of BaP in whole mussel tissues. Mussels were lyophilized and homogenized. Extraction was performed with acetone and dichloromethane using the QuEChERS method [65]. Concentration of BaP was determined using gas chromatography followed by triple quadrupole mass spectrometry (GC/MS-QqQ) [66], using BCR-682 mussel tissue as reference material. The limit of quantification in the analyses was 5 ng/g dry weight.

2.5. Determination of graphene oxide in mussel tissues and feces

Three mussels per tank were dissected, frozen in liquid nitrogen and maintained at − 40 °C until further analysis. Then 20 μm sections were obtained in a cryostat (Leica CM 3050 S) and observed under an inVia Renishaw microscope in order to get Raman spectra using a 532 nm laser. Conditions were set using the 100x objective as follows: 1–5 μm steps in the tissue, 0.2–0.4 s, 10% laser intensity, 1 accumulation and focused in 1200 nm. For each sample, serial cryotome sections were fixed in Baker's solution (formaldehyde 4% (v/v), NaCl 2% (w/v),

calcium acetate 1% (w/v)) for 15 min, rinsed in distilled water and stained 20 s in 0.1% toluidine blue to get the topographic reference of the tissue sample.

Mussels´feces were also collected and analyzed by Raman spectroscopy. Mussel feces were completely dried and placed in an aluminum foil before getting the Raman spectrum. Conditions were set using a 100x objective as follows: 100% laser intensity, 1 s, 80 accumulation and focused in 1200 nm. As reference, spectra of microalgae *Isochrysis galbana*, BaP stock solution and DMSO were obtained in the same conditions.

2.6. Cellular biomarkers in hemocytes

Hemolymph of 8 mussels per tank was withdrawn from the posterior adductor muscle and cell viability, catalase activity and DNA damage in terms of micronuclei formation were measured in hemocytes of individual mussels. Neutral red (NR) uptake was assessed according to Borenfreund & Puerner [67] with modifications explained in González-Soto et al. [60]. Catalase activity (Cat) was assessed according to Aebi [68] as modified in González-Soto et al. [60]. Protein concentration was measured following the Bradford method [69] to normalize absorbance data. Cat activity was expressed as the consumption of mM H_2O_2/min/mg protein.

The micronucleus assay was performed according to Duroudier et al. [70]. Micronucleated cells were classified following the accepted criteria for mussels: well-preserved cell cytoplasm, micronuclei not touching the main nucleus, similar or weaker staining than the main nucleus and size of micronuclei $\leq 1/3$ in comparison to the main nucleus. Other nuclear abnormalities such as binucleated cells, occurrence of nucleoplasmic bridges and nuclear buds were scored according to Pinto-Silva et al. [71] and Bolognesi & Fenech [72]. Results are reported in ‰ frequencies.

2.7. Enzyme activities in mussel tissues

Digestive gland, gills and adductor muscle of 10 mussels per tank were dissected out, frozen in liquid nitrogen and maintained at − 80 °C until further analysis. Adductor muscle was homogenized in 0.1 M potassium phosphate (KP) buffer (pH 7.2) for acetylcholinesterase (AChE) determination. Gills were cut in two halfs; one half was homogenized in 0.1 M KP buffer (pH 6.5) for glutathione *S*-transferase (GST) determination and the second half in 0.1 M KP buffer (pH 7.4) for Cat, glutathione peroxidase (GPx) and superoxide dismutase (SOD) determination. Digestive glands were divided in three parts. The first part was used for GST determination, the second for Cat, GPx and SOD, and the last piece was homogenized in 50 mM tris buffer (Tris(hydroxymethyl)-aminomethan, pH 7.8) for isocitrate dehydrogenase (IDH) determination. Tissues were homogenized in each buffer following a 1:10 proportion, tissue weight: volume of buffer.

The activity of the enzyme AChE and IDH, GST, GPx and SOD were determined as described in previous studies where some modifications of the original tecniques were made [73,74]. Briefly, AChE activity was determined according to Ellman et al. [75] at 412 nm and expressed as the production of 5,5'-dithiobis-(2-nitrobenzoic acid) in nmol/min/mg protein. IDH activity was determined according to Ellis & Goldberg [76] at 340 nm and expressed as the production of nicotinamide adenine dinucleotide phosphate (NADPH) in nmol/min/mg protein. GST activity was determined according to Habig et al. [77] at 340 nm and expressed as the production of 2,4-Dinitrochlorobenzene (CDNB) conjugates with the thiol group of glutathione in nmol/min/mg protein. Cat activity was determined as previously explained. GPx activity was determined according to Flohé & Günzler [78] at 340 nm and expressed as the consumption of NADPH in nmol/min/mg protein. SOD activity was determined according to McCord & Fridovich [79] at 550 nm and given in SOD units (1 SOD unit = 50% inhibition of the reduction of cytochrome C per mg protein). Each enzyme activity was normalized to

Table 1

Bioaccumulation of BaP in mussel soft tissues (ng/g dry weight) in control mussels and in mussels exposed to GO, GO+BaP, and BaP for 7 days. N = number of mussels is indicated. LoQ = Limit of Quantification: 5 ng/g dry weight.

Control		GO		GO+BaP		BaP	
R1	R2	R1	R2	R1	R2	R1	R2
N = 14	N = 18	N = 16	N = 14	N = 14	N = 17	N = 15	N = 14
<LoQ	<LoQ	<LoQ	<LoQ	23	28	18,700	18,400
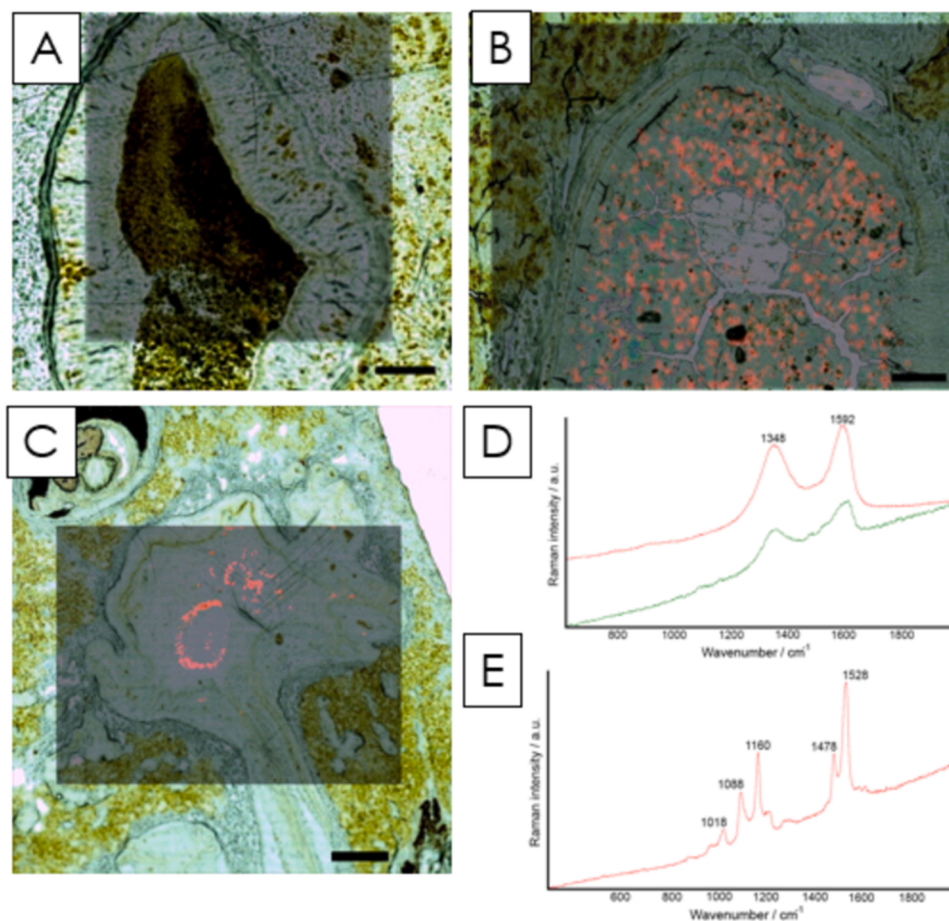
Fig. 2. A-C: Heat maps showing the detection of graphene oxide (GO) in cryostat sections of the digestive gland of different mussels; A: Control mussel, B: mussel exposed to GO for 7 days, C: mussel exposed to GO+BaP for 7 days. D: Raman spectra from the zones highlighted in red in map B (green) and the spectrum obtained for the GO stock (red). E: Raman spectrum from the map in A. Scale bars: A and B: 100 μm and C: 500 μm.

protein concentration using Bradford method [69].

2.8. Histopathology of the digestive gland

Digestive glands of 10 mussels per tank were dissected out and processed following a standard protocol for histology [80]. Briefly, tissues were fixed in 4% formalin in individual cassettes and dehydrated through a graded series of ethanol that finished in xylene using an automatic tissue processor (Leica ASP300; Leica Instruments, Wetzlar, Germany). Then, samples were embedded in paraffin and 5 μm sections were cut in a Leitz 1512 microtome (Leica Instruments, Wetzlar, Germany). Slides were dried in an oven at 37 °C (24 h) and stained with hematoxylin/eosin [81] using an autostainer XL V2.02 (Leica). Slides were mounted in DPX and analyzed under a BX51 light microscope (Olympus, Tokyo, Japan).

Vacuolization, atrophy and necrosis of the digestive tubule epithelium, fibrosis, hemocytic infiltration, aggregation of brown cells in the connective tissue and in digestive tubules and presence of parasites were assessed in the digestive gland following Villalba et al. [82], Garmendia et al. [83] and Bignell et al. [84]. The prevalence of each alteration (number of individuals showing each pathology divided by the number of individuals of each group) was calculated as percentage.

2.9. Gamete development, gonad index and histopathology of gonad

Mantle of the same animals used for the histopathological analysis of the digestive gland were dissected out and processed following the standard protocol for histology described before.

Sex ratio, gamete developmental stages and gonad index (GI) were determined. Six gamete stages were distinguished [85] and a gonad index (GI) value, ranging from 0 (resting gonad) to 5 (mature gonad), was assigned to each developmental stage as in González-Soto et al. [60], adapted from Kim et al. [86].

Oocyte atresia and necrosis, fibrosis, hemocytic infiltration, aggregation of brown cells, and occurrence of parasites were also assessed in gonads following Ortiz-Zarragoitia & Cajaraville [87]. Prevalences were
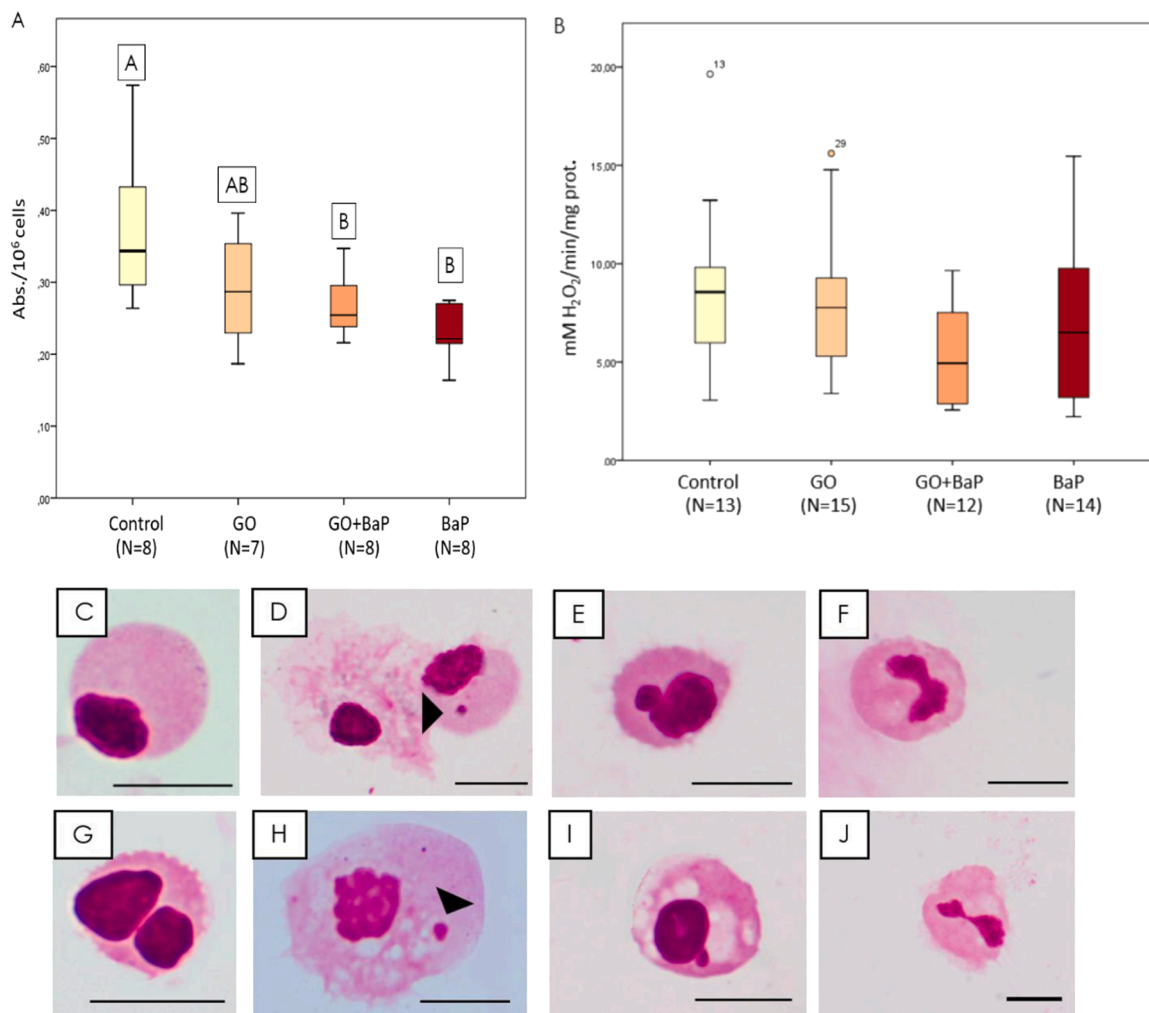
Fig. 3. A: Neutral red uptake (given as absorbance/10^6 cells); B: catalase activity (given as mM H_2O_2/min/mg prot) in hemocytes of control mussels and in mussels exposed for 7 days to GO, GO+BaP and BaP. Box-plots show median value (horizontal line), 25%−75% quartiles (box) and standard deviation (whiskers). Dots denote outliers. Letters indicate significant differences among treatments (one-way ANOVA with Tukey's post-hoc, p < 0.05); C-J: Light micrographs of mussel hemocytes during the micronucleus assay showing C) normal hemocyte of a control mussel; D) hemocyte of a mussel exposed to GO showing a micronucleus (arrow); E) hemocyte of a mussel exposed to GO showing a nuclear bud; F) binucleated cell with nucleoplasmic bridge of a mussel exposed to GO; G) binuclear hemocyte of a mussel exposed to BaP; H) hemocyte of a mussel exposed to GO+BaP showing a micronucleus (arrow); I) hemocyte of a mussel exposed to GO+BaP showing a nuclear bud; J) binucleated cell with nucleoplasmic bridge of a mussel exposed to GO+BaP. Scale bar: 10 μm.

Table 2

Frequency (‰) of micronuclei, binucleated cells, binucleated cells with nucleoplasmic bridges and nuclear buds in control mussels (N = 8) and mussels exposed for 7 days to GO (N = 7), GO+BaP (N = 6) and BaP (N = 8). Letters denote statistical differences among groups (p < 0.05 after Kruskal-Wallis test followed by Dunn's post-hoc).

	Micronuclei	Binucleated cells	Binucleated cells with nucleoplasmic bridges	Nuclear buds
Control	0 [A]	0.125 ± 0.35	2.38 ± 2.67	2.63 ± 2.13 [A]
GO	1.86 ± 1.35[B]	0.14 ± 0.38	5.43 ± 2.51	8.71 ± 2.93 [B]
GO+BaP	3.67 ± 3.08[B]	0.50 ± 0.55	6.33 ± 2.58	7.17 ± 1.72 [AB]
BaP	0.88 ± 0.83[AB]	0.63 ± 0.52	3.88 ± 2.23	5.88 ± 1.73 [AB]

calculated as for the digestive gland. In addition, intensity of oocyte atresia was assessed using a semiquantitative scale: 0- normal gonad, 1- less than a half of follicles are affected, 2- about half of follicles are affected, 3- more than half of follicles are affected and 4- all follicles are

affected [86]. Intensity was calculated as Sp/NH, where Sp is the score corresponding to the intensity of atresia and NH is the number of specimens with atresia [83].

2.10. Whole organism responses

Condition index was assessed according to Navarro et al. [88]. Soft tissues of 7 animals per tank were excised from the shells, dried at 80 °C for 24 h and weighted. Afterwards, mussel shell lengths were recorded with a Vernier caliper and condition index was calculated as tissue dry weight (g) / [shell length (cm)]^3.

2.11. Data analysis

Statistical analyses were carried out with the aid of the statistical package SPSS 24 (IBM Analytics, Armonk, NY), and the significance level was 0.05. All data sets were tested for normality and homogeneity of variance using Kolmogorov-Smirnov's and Levene's tests, respectively. Normally distributed data, which met the assumptions of homogeneity of variances, were assessed via one-way ANOVA. When significant differences were found, the Tukey's post-hoc test was used to
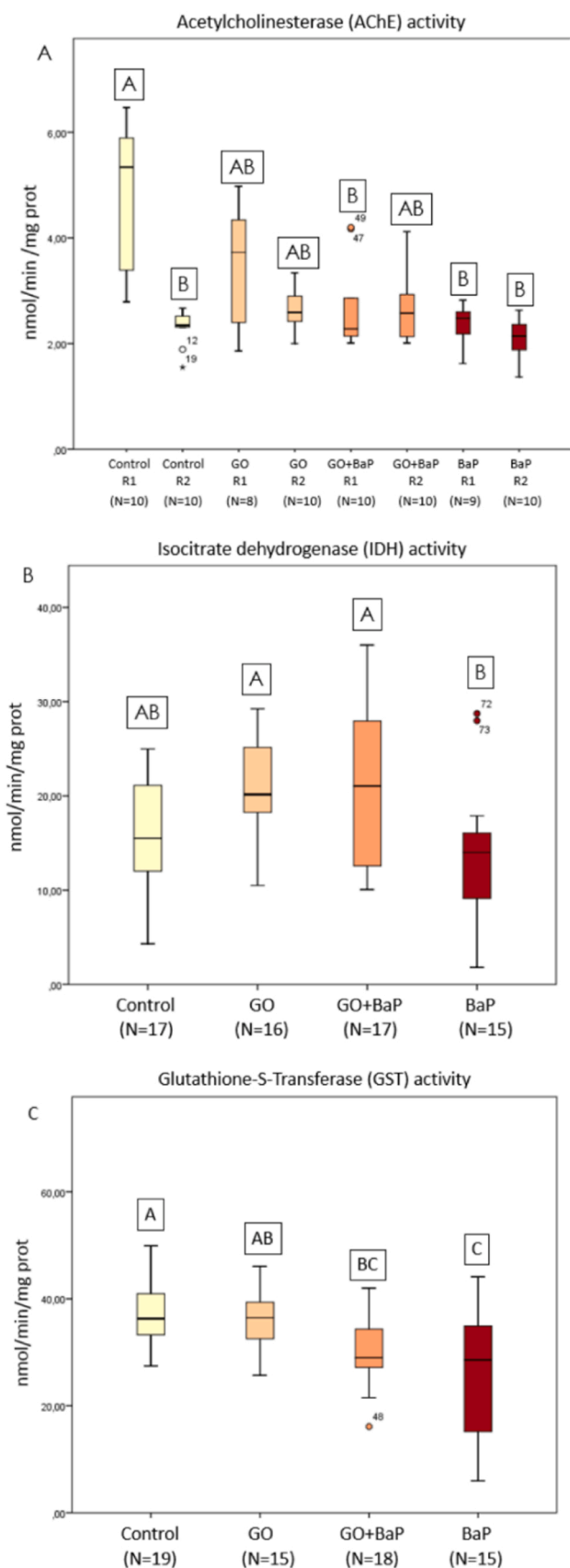
Fig. 4. Acetylcholinesterase (AChE) activity in the aductor muscle (given as nmol/min/mg prot); B) Isocitrate dehydrogenase (IDH) activity in the digestive gland (given as nmol/min/mg prot); C) Glutathione-S-Tramsferase (GST) activity in the digestive gland (given as nmol/min/mg prot) control mussels and in mussels exposed for 7 days to GO, GO+BaP and BaP. Box-plots show median value (horizontal line), 25%– 75% quartiles (box) and standard deviation (whiskers). Dots denote outliers. Letters denote statistical differences among means (Kruskal-Wallis test followed by Dunn's post-hoc in AChE and GST and one-way ANOVA followed by Tukey's post-hoc in IDH, $p < 0.05$).

identify significant different treatments. Data which did not met the above assumptions were analyzed by the one-way Kruskal-Wallis test, followed by the Dunn's post-hoc test when significant differences were found. For histopathological data expressed as percentages, the X^2 test was used [89]. When no differences were found between the two replicate tanks, data sets were mixed and displayed as: Control, GO, GO+BaP, BaP. However, when differences were found between replicates, data sets were maintained separate and displayed as: Control R1, Control R2, GO R1, GO R2, GO+BaP R1, GO+BaP R2, BaP R1, BaP R2.

3. Results

3.1. Bioaccumulation of BaP

BaP concentration in control mussels and in mussels exposed to GO was below the detection limit (Table 1). BaP was bioaccumulated in mussels exposed to GO+BaP (23–28 ng/g dry weight), but especially in mussels exposed to BaP (18,400–18,700 ng/g dry weight) (Table 1). In water, BaP was detected only in the tanks exposed to BaP alone.

3.2. Determination of graphene oxide in mussel tissues and feces

GO was detected only in the lumen of the digestive tract of mussels exposed to both GO and GO+BaP (Fig. 2), indicating that even if GO was internalized, it was not accumulated in the rest of mussel tissues after 7 days of exposure. Accordingly, GO was detected in feces of mussels exposed to GO and GO+BaP from day one of exposure (Fig. S2). Spectra of microalgae *Isochrysis galbana*, BaP stock solution and DMSO were not observed in mussel tissues or feces.
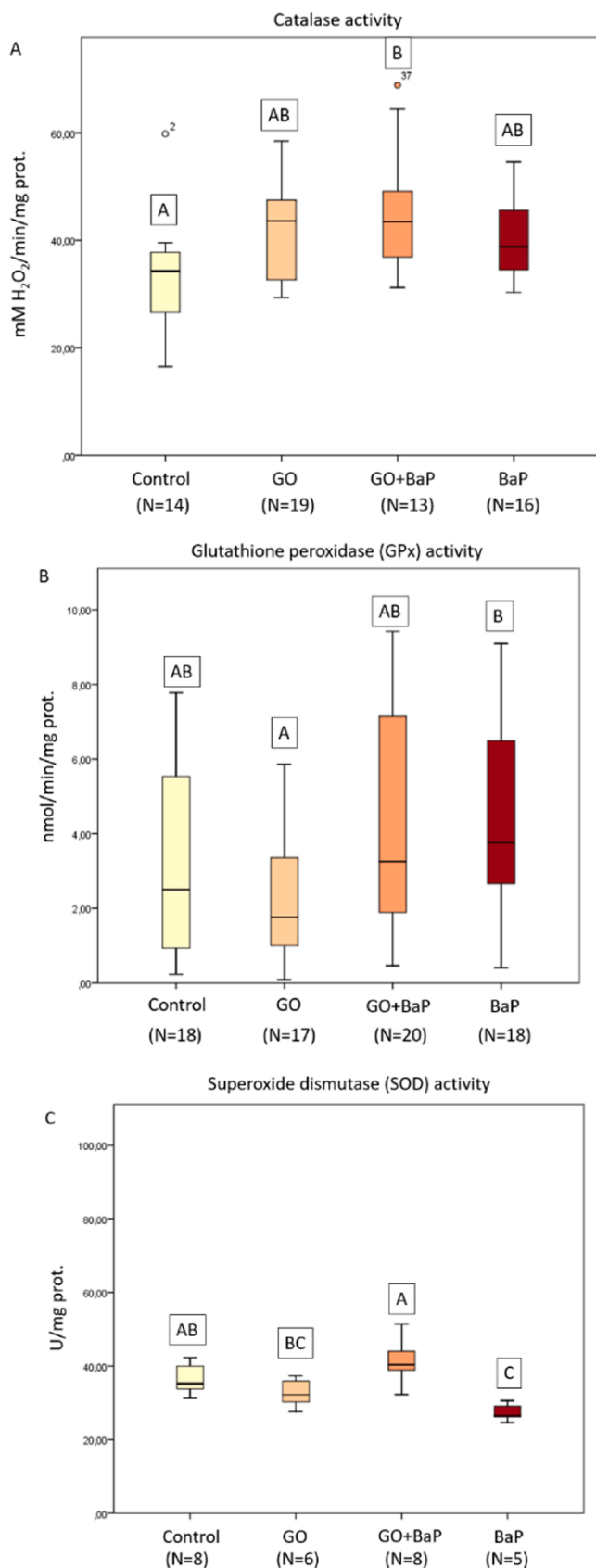
3.3. Cellular biomarkers in hemocytes

Viability of hemocytes decreased in mussels exposed to GO+BaP and BaP in comparison to controls (Fig. 3A). No differences were observed among groups in the activity of catalase (Cat) (Fig. 3B).

Regarding genotoxicity, higher micronuclei frequency was observed in hemocytes of mussels exposed to GO and GO+BaP in comparison to controls (Table 2, Fig. 3D, G). In addition, higher frequency of nuclear buds was observed in hemocytes of mussels exposed to GO than in control mussels (Table 2, Fig. 3E, H). No differences were observed among groups in binucleated cells (Table 2, Fig. 3J) and binucleated cells with a nucleoplasmic bridge (Table 2, Fig. 3F, I).

3.4. Enzyme activities in mussel tissues

There were statistically significant differences in the activity of acetylcholinesterase (AChE) between replicates and thus, data were treated separately (Fig. 4A). Activity of AChE was lower in one of the replicates exposed to GO+BaP (R1) and in both replicates exposed to BaP in comparison to one of the control replicates (R1) (Fig. 4A). Inhibition of isocitrate dehydrogenase (IDH) was observed in mussels exposed to BaP in comparison to mussels exposed to GO and GO+BaP (Fig. 4B). Similarly, inhibition of Glutathione-S-Transferase (GST) was observed in the digestive gland of mussels exposed to GO+BaP and BaP in comparison to control mussels (Fig. 4C), while no response was observed in gills (Fig. S3A).

(caption on next column)

Regarding antioxidant enzymes, induction of Cat activity was observed in the digestive gland of mussels exposed to GO+BaP in comparison to controls (Fig. 5A), but no response was observed in gills (Fig. S3B). No differences were found in the activity of glutathione peroxidase (GPx) in the digestive gland (Fig. S3C), but inhibition was observed in gills of mussels exposed to GO in comparison to mussels exposed to BaP (Fig. 5B).

Superoxide dismutase (SOD) was inhibited in the digestive gland of mussels exposed to BaP in comparison to control mussels and mussels exposed to GO+BaP, while induction of SOD was observed in mussels exposed to GO+BaP in comparison to mussels exposed to GO and BaP (Fig. 5C). However, no clear trend was observed in gills (Fig. S3C).

3.5. Histopathology of digestive gland

Statistical differences were found between replicates for some histopathological alterations. In those cases data sets for the two replicates were treated separately (Table 3). Fibrosis (Fig. 6A) was widespread in all mussels including controls. All groups showed high prevalences, significantly higher in BaP R1 than in GO R1 (Table 3). Prevalence of hemocytic infiltration (Fig. 6B) was similar in control R2 and all exposure groups but it was significantly higher in the GO R2 group than in control R1 (Table 3). Overall, aggregation of brown cells (Fig. 6C, D) were more frequent in exposed groups than in controls, at least in one of the replicates (Table 3). Aggregation of brown cells in the connective tissue was significantly higher in mussels exposed to GO, GO+BaP and BaP than in controls (Table 3) while in the digestive tract epithelium, it was significantly higher in GO R2 and GO+BaP R1 than in control R1 (Table 3). In addition, aggregation of brown cells in the digestive tract epithelium was significantly higher in GO+BaP R1 than in GO R1 (Table 3).

Areas of necrosis of digestive tubule epithelium were found in both control and exposed mussels. Prevalence of necrosis was significantly higher in GO+BaP R2 and BaP R2 compared to control R2 (Table 3). Necrosis of digestive tubule epithelium appeared to be associated to the occurrence of an intracellular ciliated protozoan. It was found in the digestive epithelium of mussels of all experimental groups, with its highest prevalence in controls, especially in comparison to mussels exposed to BaP (Table 3). In addition, the protozoan *Nematopsis* sp. was the most common parasite in the digestive gland. It appeared in the connective tissue of almost all mussels, with high prevalences in all the replicates (Table 3). Other parasites such as *Mytilicola intestinalis* were also observed in the digestive gland of some mussels, but with low prevalences (Table 3).

3.6. Gamete development, gonad index and histopathology of mussel gonad

Mussels from different groups were in a similar gamete development stage. Spawning was the predominant stage (Fig. S4) as expected for the experimental period. There were no differences in the sex ratio and gonad index among groups (Fig. S4).

Fibrosis (Fig. 6F), hemocytic infiltration (Fig. 6G) and aggregation of brown cells (Fig. 6H) were widely observed in the gonad of both control and exposed mussels. Prevalence of fibrosis was significantly higher in BaP R2 mussels than in Control R2 mussels (Table 4). Hemocytic

(caption on next column)

Table 3

Prevalence of histopathological alterations in the digestive gland of both replicates (R1 and R2) of control mussels and mussels exposed to GO, GO+BaP and BaP for 7 days. Data are shown in percentages of 10 mussels per experimental replicate tank. Letters denote statistical differences for each alteration (X^2 test, p < 0,05).

		Inflammatory responses				Parasites		
	Fibrosis	Hemocytic infiltration	Brown cells in the connective tissue	Brown cells in the digestive tract epithelium	Necrosis of digestive tubule epithelium	Intracellular ciliated protozoan	*Nematopsis sp.*	*Mytilicola intestinalis*
Control R1	90[AB]	10[A]	0[A]	10[A]	50[AB]	80[A]	80	10
Control R2	90[AB]	40[AB]	30[A]	30[ABC]	80[A]	70[A]	100	20
GO R1	80[A]	50[AB]	60[B]	20[AB]	50[AB]	60[AB]	90	10
GO R2	60[AB]	60[B]	60[B]	60[CB]	60[AB]	30[AB]	100	0
GO+BaP R1	90[AB]	40[AB]	60[B]	70[C]	60[AB]	60[AB]	80	20
GO+BaP R2	90[AB]	50[AB]	40[B]	20[AB]	30[B]	40[AB]	80	10
BaP R1	100[B]	40[AB]	70[B]	10[A]	80[A]	40[B]	90	10
BaP R2	90 A[B]	50[AB]	60[B]	30[ABC]	20[B]	40[B]	70	20

infiltration occurred both in the connective tissue and within the gonad follicles and prevalences were higher in GO+BaP R1 and BaP R2 than in both control replicates and in GO R1 (Table 4). Aggregation of brown cells, both in the connective tissues and gonad follicles, was higher in mussels exposed to GO and to BaP than in controls (Table 4). However, the main histopathological alteration observed was oocyte atresia (Fig. 6F) with prevalences over 75% in all control and exposed groups (Table 4). Control mussels showed low intensity of atresia which can be linked to the developmental stage of the gonad (Table 4, Fig. S4). On the other hand, stages 2 and 3 of oocyte atresia were only recorded in exposed mussels and the highest intensity was found in mussels exposed to GO+BaP (Table 4). *Nematopsis sp.* protozoan was found in the connective tissue of the gonad of almost all mussels (Table 4).

3.7. Whole organism responses

No differences were recorded among groups in mussel condition index (Fig. S5).

4. Discussion

In this work, the toxic effects of short-term (7 days) exposure to GO alone (500 μg/L) and to GO with sorbed BaP (500 μg/L GO incubated with 100 μg/L BaP) has been assessed using a wide selection of biological responses, from molecular to organism levels. For comparison, the effects of exposure to BaP alone at a concentration of 96.7 μg/L, equivalent to that sorbed in GO+BaP preparations [63], were also assessed. In parallel, the fate of GO nanoplatelets in mussels was studied by Raman spectroscopy, as well as BaP bioaccumulation.

After 20 h of exposure, BaP or GO could not be detected in the water of tanks exposed to GO+BaP, suggesting that mussels had uptaken the GO nanoplatelets with sorbed BaP. Little is known about the desorption dynamics of PAHs from GO and other GFNs in the marine environment. In aqueous solutions, adsorption of phenanthrene into magnetic graphene is mostly irreversible [90]. The stability of GO with sorbed BaP could explain that BaP was undetectable in water in GO+BaP tanks as mussels would internalize BaP adsorbed into GO nanoplatelets. However, the concentration of BaP bioaccumulated in mussels was much lower in mussels exposed to GO+BaP compared to those exposed to dissolved BaP. Sanchis et al. [41] reported that the Trojan horse effect is more likely to occur with organic pollutants that present an intermediate affinity to carbon-based NMs, than with non polar compounds showing aromatic rings such as BaP, as the most non polar compounds would be irreversibly bound to the carbon-based NMs decreasing their bioavailability. Alternatively, it could be that BaP bioaccumulation was low in mussels exposed to GO+BaP because of the excretion of GO nanoplatelets with sorbed BaP. This idea is supported by the detection of GO

in feces of mussels exposed to GO and to GO+BaP.

At studying the stability of GO in tanks with and without oysters, Khan et al. [34,91] concluded that the animals were actively removing the GO from the water, in line with our results. Filtration is the common pathway for the internalization of different NMs during the feeding process of filter-feeding organisms such as mussels. After a first contact with the gills, NM aggregates are ingested and, depending on their size, they can be accumulated in the digestive gland and/or translocated to hemolymph and then distributed to other organs [92]. In the present work GO was not detected in gills, probably due to the short contact between GO and gills. This could explain the lack of effects on enzyme activities studied in gills of mussels exposed to GO and GO+BaP in comparison to controls. Presence of GO was confirmed through Raman spectroscopy in the lumen of the digestive tract and feces of mussels exposed to both GO and GO+BaP, suggesting that GO tends to accumulate in organs related with food intake, as previously reported by Josende and colleagues [93]. The presence of GO in the digestive tract has been previously reported in exposures to other aquatic invertebrates, such as nematodes [36] and crustaceans [93–98], but not in bivalves. To the best of our knowledge this is the first time that the presence of GO in the digestive tract of bivalves was confirmed through Raman spectroscopy. As the digestive gland is one of the most important organs in mussels, responsible for intracellular digestion and also for antioxidant defense and pollutant sequestration and detoxification, significant damages in this organ could lead to impact at the organism level [92,99,100]. GO could then be translocated from the digestive system to the rest of organs [101,102]. However, Bortolozzo et al. [36] observed that carboxyl groups in GO edges can avoid permeability of GO nanoplatelets through the intestine in nematodes. This could explain the presence of GO in feces after each digestive cycle and the absence of GO out of the digestive tract in this work, although there is yet no conclusive data on the distribution and excretion strategies for GFNs inside animal bodies [5].

Even though GO was not detected in hemocytes by Raman spectroscopy, cytotoxicity occurred in hemocytes of mussels exposed to GO+BaP and BaP with respect to controls. Further, genotoxic effects were observed in hemocytes of mussels exposed to GO and GO+BaP in comparison to controls. DNA damage has been previously reported in other organisms exposed to GO [103–106], but there is a single work reporting genotoxicity of GFNs to mussels [107]. Genotoxicity may be provoked by the physical damage caused by nanoplatelets and/or through oxidative stress [93,101]. In most publications the comet assay has been used to measure genotoxicity after exposure to GFNs, but DNA strand breaks determined by the comet assay can be reversible [108]. Flasz et al. [105] reported that DNA damage measured in crickets *Acheta domesticus* by the comet assay after 5 and 25 days of GO exposure was completely reversed after 10 days of depuration. On the other hand,
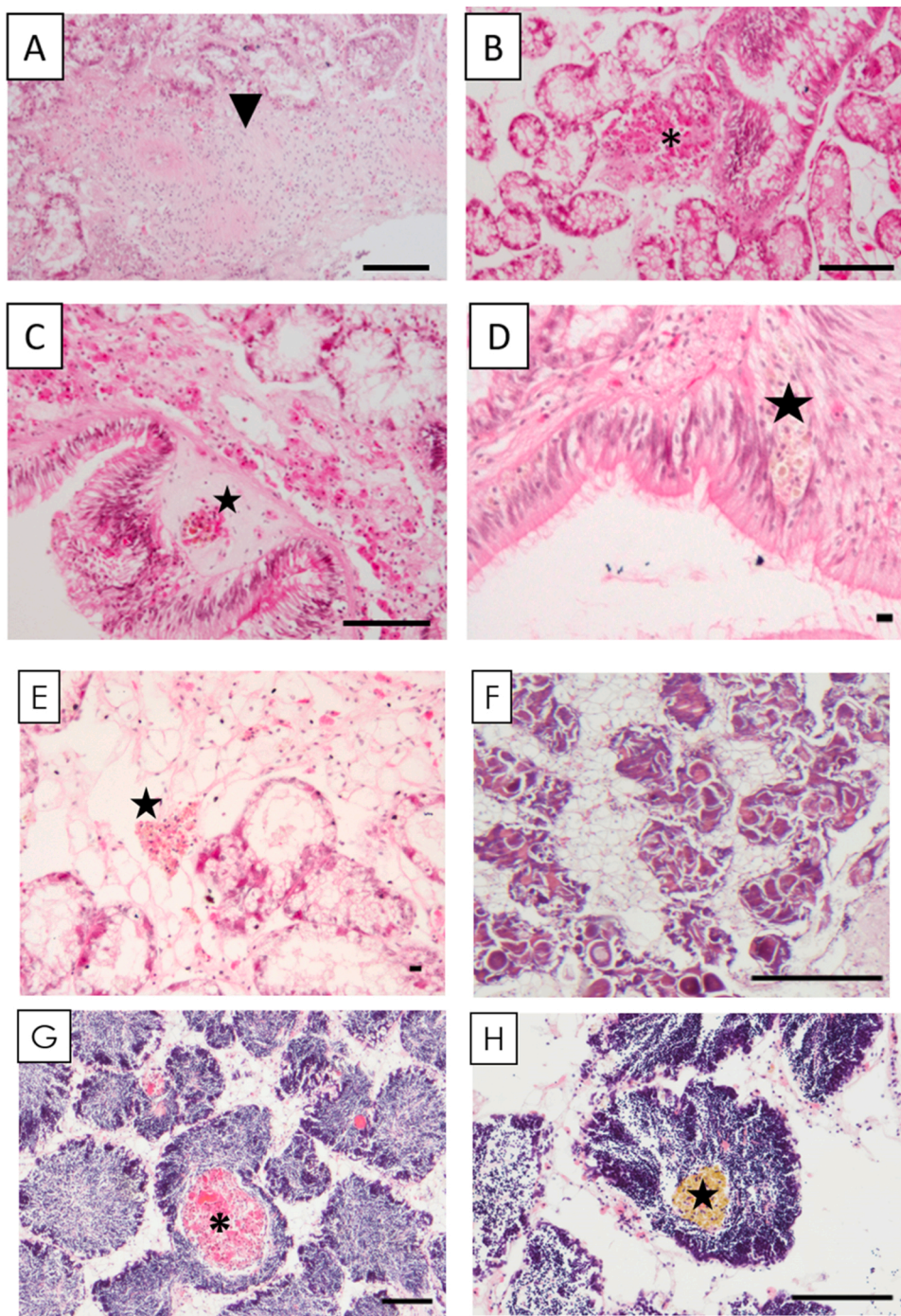
Fig. 6. Light micrographs of mussel paraffin sections showing histopathological alterations in mussels digestive gland and gonads: A) mussel after 7 days of exposure to GO+BaP showing fibrosis in the connective tissue (arrow head); B) mussel after 7 days of exposure to GO+BaP showing hemocytic infiltration (*); C) mussel after 7 days of exposure to GO showing aggregation of brown cells in the epithelium of the digestive tract (star); D) mussel after 7 days of exposure to GO+BaP showing aggregation of brown cells in the epithelium of the digestive tract (star); E) mussel after 7 days of exposure to GO showing aggregation of brown cells in the connective tissue (star); F) mussel after 7 days of exposure to GO+BaP showing oocyte atresia; G) mussel after 7 days of exposure to BaP showing hemocytic infiltration within a male follicle (*); H) mussel after 7 days of exposure to BaP showing aggregation of brown cells within a male follicle (star). Scale bar: A, B, C, G, H: 100 μm; D,E: 10 μm; F: 500 μm.

micronuclei frequency measured in this work assesses DNA damage that remains after cell division [5,109]. Thus, the increased occurrence of micronuclei in hemocytes of mussels exposed to GO+BaP and of nuclear buds in those exposed to GO acquires a great environmental relevance.

Due to its link with genotoxicity, oxidative stress is one of the most studied biomarkers after organism exposure to GO. In this work no differences in hemocyte Cat activity were observed among exposure groups. This could be because exposure was not enough to induce hemocyte Cat activity or because the antioxidant system of hemocytes already reached its maximum after 7 days of exposure. Many antioxidant enzymes follow a bell-shaped curve whereby activation of the synthesis of a specific enzyme causes an initial increase in the activation of the enzyme followed by its decrease, caused by the increased

catabolic rate or direct inhibitory effects of toxic chemicals on the enzyme molecules [110]. The fact that viability was reduced in hemocytes of mussels exposed to GO+BaP supports the idea that probably after 7 days of exposure hemocytes were not able to overcome ROS production by inducing Cat activity, thus leading to oxidative stress and non-reversible DNA damage in hemocytes.

In agreement with the occurrence of GO in the lumen of the digestive tract in mussels exposed to GO and GO+BaP, the digestive gland was more sensitive than the gills in terms of effects on biotransformation (GST) and antioxidant enzyme activities Cat and SOD. Inhibition of GST and induction of Cat enzyme activities were observed in the digestive gland of mussels exposed to GO+BaP with respect to the controls. Similarly, the activity of SOD was induced in the digestive gland of

Table 4
Prevalence of histopathological alterations in gonad of both replicates (R1 and R2) of control mussels and mussels exposed to GO, GO+BaP and BaP for 7 days. Data are shown in percentages of 10 mussels per replicate tank, except for atresia which was calculated based on the number of females in each group (Fig. S4). The intensity of oocyte atresia is given by an index calculated as the average of the intensities based on a scale from 0 to 4. Letters denote statistical differences for each alteration (X^2 test, $p < 0,05$).

	Fibrosis	Inflammatory responses		Oocyte atresia		Parasites
		Hemocytic infiltration	Aggregation of brown cells	Prevalence	Intensity	*Nematopsis sp.*
Control R1	44.44[AB]	44.44[BC]	22.22 [A]	100	1 [A]	88.89
Control R2	30[A]	40[BC]	30 [A]	100	1 [A]	80
GO R1	60[AB]	30 [C]	50[BC]	100	1 [A]	70
GO R2	44.44[AB]	77.78[ABC]	66.67[BC]	100	1.4[AB]	55.56
GO+BaP R1	44.44[AB]	88.89[AE]	33.33[ABC]	100	1.43[B]	66.67
GO+BaP R2	66.67[AB]	55.56[ABC]	33.33[ABC]	100	1.75[B]	66.67
BaP R1	60[AB]	50[ABC]	50[B]	75	0.75 [A]	80
BaP R2	77.78[B]	100[DE]	33.33[B]	100	1.33 [A]	88.89
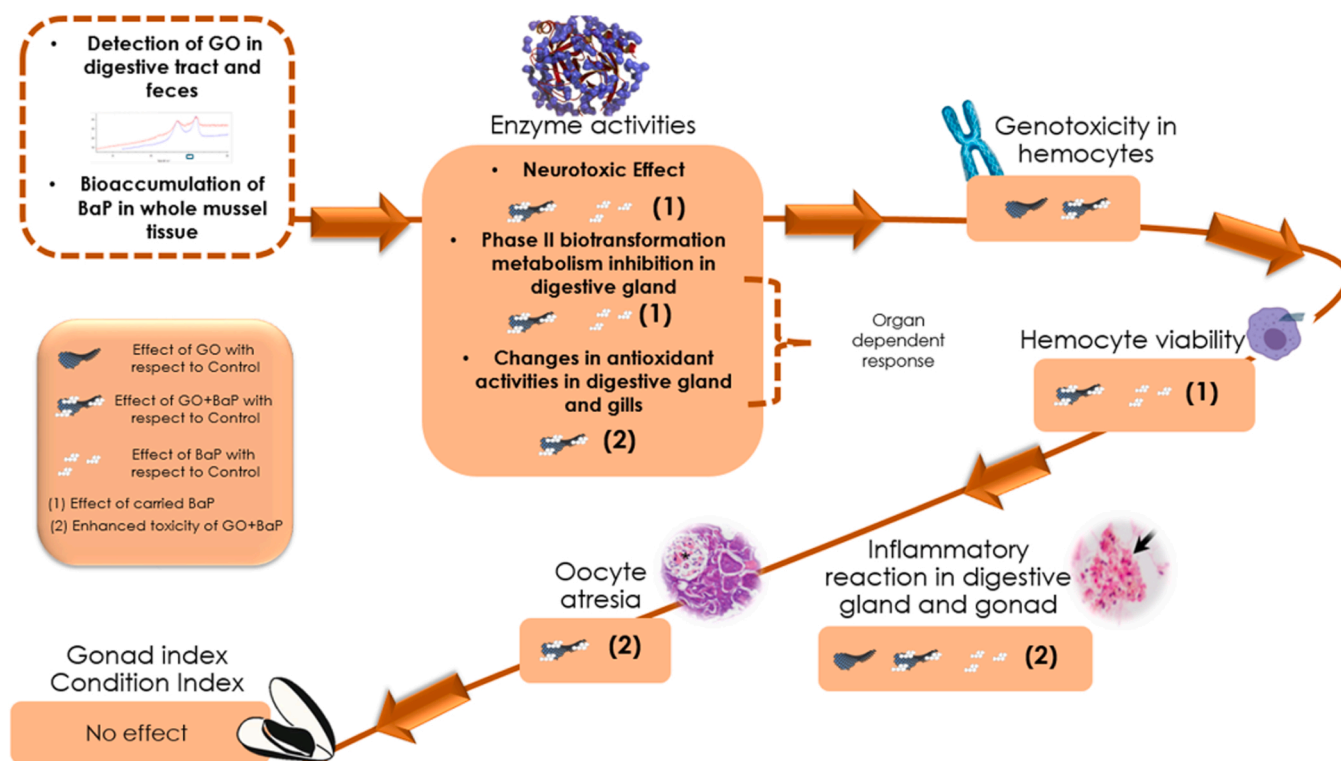
Fig. 7. Summary of results obtained at different biological levels.

mussels exposed to GO+BaP compared to those exposed to GO. Barranger et al. [111,112] and Moore et al. [100] also reported a higher impact in terms of altered enzyme activities in the digestive gland in comparison to the rest of organs in mussels exposed to carbon-based NMs and BaP. Furthermore, it has been reported that Cat and SOD are related to each other and can be activated by BaP exposure alone or in combination with other pollutants [113]. In the present study, exposure to dissolved BaP provoked inhibition of GST, SOD and AChE with respect to controls, and also inhibition of IDH with respect to GO and GO+BaP groups and induction of gill GPx with respect to GO groups. These results suggest that effects observed in mussels exposed to GO+BaP could be at least partially due to BaP carried out by GO nanoplatelets to mussels.

In the case of mussels exposed to GO alone, there were no alterations in the enzyme activities related to neurotoxicity, aerobic metabolism, biotransformation or oxidative stress in comparison to control mussels. There are no conclusive results related to the oxidative stress caused by GFNs in bivalves yet. For example, in the study of Coppola et al. [113] after 28 days of exposure of mussels to GO functionalized with

polyethyleneimine (GO-PEI), activities of SOD, CAT and GPx were induced with respect to controls. However, such results were not reproduced in a subsequent report by Coppola et al. [115]. Many works have pointed out that the complex toxicity profiles of GFNs could be related to the reactivity of nanoplatelets used in each study, which depend on the specific molecular structure of the surface of the nanoplatelets and especially on their oxygen content [4,17,29,36]. Small variations in the structure of GO, which are inevitable during the production of different batches, would alter its toxicity.

At tissue level, impact of graphene [116] and GO-PEI [114] have been previously reported in terms of loss of tissue and digestive tubule atrophy, respectively. Bi et al. [117] also reported thinning of the digestive tubule epithelium and loss of digestive cells in clams *Corbicula fluminea* after 28 days of exposure to GO. In the present study, a high prevalence of necrosis of the digestive tubule epithelium was found, possibly due to the widespread occurrence of an intraepithelial ciliated protozoan parasite, but prevalence significantly increased in one GO+BaP replicate and one BaP replicate compared to one control replicate. Most importantly, non-specific inflammatory responses such

Table 5

Summary of results obtained comparing the toxicity profile of GO+BaP with respect to controls and to GO or BaP alone. BC: brown cell aggregations, CAT: catalase, CT: connective tissue, DG: digestive gland, DT: digestive tract GST: glutathion-S-transferase, SOD: superoxide dismutase. X: does not apply.

	Effect of GO+BaP with respect to Controls	Effect of GO+BaP with respect to GO	Effect of GO+BaP with respect to BaP	Same effect of GO+BaP with respect to control observed in in GO or BaP with respect to control	Conclusion
BaP bioaccumulation	↑	↑	↓	none	GO protects against BaP accumulation
Occurrence of GO	↑	=	X	GO	No effect of carried BaP
Hemocyte viability	↓	=	=	BaP	Effect of carried BaP
Genotoxicity	↓ (1 R)	=	=	GO	Effect of GO
Neurotoxicity	↓	=	=	BaP	Effect of carried BaP
GST DG	↓	=	=	BaP	Effect of carried BaP
CAT DG	=	↑	↑	none	Enhanced effect of GO+BaP
SOD DG	↑	↑	↑	none	Enhanced effect of GO+BaP
BC in CT of DG	↑	=	=	GO and BaP	All cause same effect
BC in DT of DG	↑ (1 R)	↑ (1 R)	↑ (1 R)	GO (1 R)	Enhanced effect of GO+BaP
Oocyte atresia	↑	↑	↑	none	Enhanced effect of GO+BaP

as hemocytic infiltration and accumulation of brown cells in the connective tissue and digestive tract epithelium of the digestive gland were found in mussels exposed to GO and GO+BaP, as well as in mussels exposed to BaP for brown cells in the digestive gland connective tissue. Similarly, non-specific inflammatory responses have been reported in multiple cell lines [118], fishes [119] and oysters [34] after exposure to GO. Acute inflammation responses and chronic injury could interfere with normal physiological functions in organs [5]. Therefore, long-term exposure experiments of bivalves to GO alone and with associated pollutants, including a recovery period, are necessary to decipher whether these damages are reversible or not.

Similar to results in the digestive gland, prevalence of non-specific hemocytic infiltration increased in the gonad of mussels exposed to GO+BaP in comparison to controls and GO, and in one BaP replicate compared to controls, GO+BaP and GO exposure groups. Prevalence of brown cell aggregations was also higher in the gonad of mussels exposed to GO and BaP compared to controls. Further, a higher intensity of oocyte atresia was observed in mussels exposed to GO+BaP in comparison to controls and mussels exposed to BaP. The appearance of atresia in early gametogenic stages has been related with the presence of pollutants such as PAHs in mussels [87,120,121]. BaP exposure can cause alterations in sex hormones, disintegration of cell membranes, DNA damage, inhibition of ovarian development and increment of atretic follicles in bivalves [122–124]. Moreover, developing and mature stages of the gonad are the most susceptible to BaP exposure [123]. In addition, GO can also provoke degenerative effects in gonads. Bi et al. [117] reported that clams exposed to GO alone or in combination to perfluorooctane sulfonate (PFOS) showed smaller oocytes. Dziewiecka et al. [104] suggested that GO might cause degenerative changes in the female gonad due to its sharp edges, although in the present work direct interaction of nanoplatelets with oocytes was unlikely, according to Raman results. In summary, the most severe atresia observed in mussels exposed to GO+BaP was possibly a result of synergistic effects of both GO nanoplatelets and adsorbed BaP.

Neurotoxicity was observed in terms of inhibited AChE activity in mussels exposed to one GO+BaP replicate in comparison to control mussels and in those exposed to BaP in comparison to controls. While it is known that BaP can display neurotoxic effects on bivalves [113, 125–127], the neurotoxic potential of GFNs is not clear. Alterations of AChE activity and several neurotransmitters have been observed in bivalves and fishes exposed to different GFNs [101,114,128], whereas the opposite has also been reported [35,115,129].

Overall, in this work the toxicity of GO+BaP appeared to be explained by effects of GO for certain biological responses (genotoxicity and non-specific inflammatory responses in digestive gland and gonad) and by effects of BaP carried by GO for other responses (decrease in hemocyte viability, changes in enzyme activities and inflammatory and degenerative alterations in digestive gland and gonad) (Fig. 7, Table 5). Most of the alterations observed after BaP exposure have been previously reported: decrease in hemocyte viability [130], inhibition of AchE activity [125,126], inhibition of GST in digestive gland [131,132] and histopathological damage in gonad [122–124]. On the other hand, in some biomarkers impact was only observed in mussels exposed to GO+BaP in comparison to the controls (Fig. 7, Table 5). This was the case of Cat induction in digestive gland and oocyte atresia. Finally, in other cases, toxicity of GO+BaP was enhanced in comparison to GO and/or BaP alone (Fig. 7, Table 5). These results highlight the complexity of the interactions of GFNs with sorbed BaP in marine mussels (Table 5).

5. Conclusions

In conclusion, after a short exposure of 7 days to environmentally relevant concentrations of GO and GO with sorbed BaP, GO was observed in the lumen of the digestive tract and feces of mussels suggesting that GO was internalized via ingestion and rapidly excreted. BaP

was bioaccumulated in mussels exposed to GO with sorbed BaP, pointing to a carrier role of GO towards BaP. However, the extent of BaP bioaccumulation was much higher in mussels exposed to BaP alone compared to those exposed to GO+BaP at equivalent exposure concentrations of BaP. Thus, it appeared that GO nanoplatelets protected mussels against BaP bioaccumulation, as reported in previous studies with other carbon-based NMs and BaP in mussels [100,111,112]. Regarding the toxicological impact of exposure to GO+BaP in mussels, complex patterns of interaction between GO and BaP emerged which differed depending on the biological endpoint studied. Some responses could be attributted to the effects caused by GO alone but most responses seemed to be due to a Trojan horse effect, including 1) effects of BaP carried onto GO nanoplatelets, and 2) enhanced toxic effects of GO+BaP compared to GO and/or BaP alone or to controls but not to GO and/or BaP alone, (Table 5). This work underlines the necessity of studying GFNs toxicity in combination with other pollutants. Experiments of exposure to single GFNs could lead to an underestimation of their possible impact in the environment, where these NMs would appear together with other environmental pollutants. Further work is needed to address the potential hazard that GFNs may pose in the marine environment, particularly at long term.

CRediT authorship contribution statement

N.G.-S., E.B. and M.P.C. designed the experiment; N.G.-S. performed the experiment and laboratory work, data acquisition, treatment and statistical analysis, prepared the graphs and tables, and wrote a first draft of the manuscript; N.B. contributed to the histopathological analysis; M.I. contributed to data acquisition and treatment of Raman spectroscopy; L.G. supervised the laboratory work on enzyme activities; E.B. and M.P.C. supervised all laboratory work, data treatment and analysis; interpretation and discussion of results; N.B, E.B., L.G. and M.P.C. revised the manuscript; M.P.C. designed and supervised the overall project, obtained funding and produced the final manuscript.

Declaration of Competing Interest

The authors declare that they have no known competing financial interests or personal relationships that could have appeared to influence the work reported in this paper.

Data Availability

Data will be made available on request.

Acknowledgements

Environmental Implication

The increasing production and use of graphene oxide (GO) could lead to its entry into the ocean. There, GO can adsorb persistent organic pollutants, like benzo(a)pyrene (BaP) and facilitate its transfer to organisms (the so-called Trojan horse effect). This is the first work that studied this effect for GO and BaP in bivalves, using an environmentally relevant concentration of GO. Complex patterns of interaction between GO and BaP were observed depending on the endpoint studied. This work contributes to understand the hazards posed by graphene nanomaterials in an environmentally realistic scenario.

Appendix A. Supporting information

Supplementary data associated with this article can be found in the online version at doi:10.1016/j.jhazmat.2023.131280.

References

[1] Nel, A., Xia, T., Mädler, L., Li, N., 2006. Toxic potential of materials at the nanolevel. Science 311, 622–627.

[2] EU COM, Commission Recommendation of 18 October 2011 on the definition of nanomaterial Text with EEA relevance OJ L 275, 20.10.2011, p. 38–40 (EN). http://data.europa.eu/eli/reco/2011/696/oj

[3] Novoselov, K.S., Fal, V.I., Colombo, L., Gellert, P.R., Schwab, M.G., Kim, K., 2012. A roadmap for graphene. Nature 490, 192–200.

[4] Peng, Z., Liu, X., Zhang, W., Zeng, Z., Liu, Z., Zhang, C., Liu, Y., Shao, B., Liang, Q., Tang, W., Yuan, X., 2020. Advances in the application, toxicity and degradation of carbon nanomaterials in environment: a review. Environ Int 134, 105298.

[5] Ou, L., Song, B., Liang, H., Liu, J., Feng, X., Deng, B., Sun, T., Shao, L., 2016. Toxicity of graphene-family nanoparticles: a general review of the origins and mechanisms. Part Fibre Toxicol 13, 57.

[6] Ren, W., Cheng, H.M., 2014. The global growth of graphene. Nat Nanotechnol 9, 726–730.

[7] Yao, W., Zhou, S., Wang, Z., Lu, Z., Houc, C., 2020. Antioxidant behaviors of graphene in marine environment: a first-principles simulation. Appl Surf Sci 499, 143962.

[8] Kabiri, S., Degryse, F., Tran, D.N., da Silva, R.C., McLaughlin, M.J., Losic, D., 2017. Graphene oxide: a new carrier for slow release of plant micronutrients. ACS Appl Mater Interfaces 9, 43325–43335.

[9] Le, V.T., Almomani, F., Vasseghian, Y., Vilas–Boas, J.A., Dragoi, E.N., 2021. Graphene-based nanomaterial for desalination of water: a systematic review and meta-analysis. Food Chem Toxicol 148, 111964.

[10] Ahmad, S.Z.N., Salleh, W.N.W., Ismail, A.F., Yusof, N., Yusop, M.Z.M., Aziz, F., 2020. Adsorptive removal of heavy metal ions using graphene- based nanomaterials: Toxicity, roles of functional groups and mechanisms. Chemosphere 248, 126008.

[11] Scott, A., 2016. Graphene's global race to market. Chem Eng N 94, 28–33.

[12] De Marchi, L., Pretti, C., Gabriel, B., Marques, P.A., Freitas, R., Neto, V., 2018. An overview of graphene materials: properties, applications and toxicity on aquatic environments. Sci Total Environ 631, 1440–1456.

[13] Arvidsson, R., Baun, A., Furbe, A., Hansen, S.F., Molander, S., 2018. Proxy measures for simplified environmental assessment of manufactured nanomaterials. Environ Sci Technol 52, 13670–13680.

[14] Collins R. 2021. Graphene Market & 2D Materials Assessment 2021–2031. IDTechEx, 9781913899219.

[15] Dreyer, D.R., Park, S., Bielawski, C.W., Ruoff, R.S., 2010. The chemistry of graphene oxide. Chem Soc Rev 39, 228–240.

[16] Chen, D., Feng, H., Li, J., 2012. Graphene oxide: preparation, functionalization, and electrochemical applications. Chem Rev 112, 6027–6053.

[17] Malina, T., Maršálkova, E., Holá, K., Zbořil, R., Maršálek, B., 2020. The environmental fate of graphene oxide in aquatic environment complete mitigation of its acute toxicity to planktonic and benthic crustaceans by algae. J Hazard Mater 399, 123027.

[18] Zhao, J., Wang, Z., White, J.C., Xing, B., 2014. Graphene in the aquatic environment: adsorption, dispersion, toxicity and transformation. Environ Sci Technol 48, 9995–10009.

[19] He, K., Chen, G., Zeng, G., Peng, M., Huang, Z., Shi, J., Huang, T., 2017. Stability, transport and ecosystem effects of graphene in water and soil environments. Nanoscale 9, 5370–5388.

[20] Avant, B., Bouchard, D., Chang, X., Hsieh, H.S., Acrey, B., Han, Y., Spear, J., Zepp, R., Knightes, C.D., 2019. Environmental fate of multiwalled carbon nanotubes and graphene oxide across different aquatic ecosystems. NanoImpact 13, 1–12.

[21] Moore, M.N., 2006. Do nanoparticles present ecotoxicological risks for the health of the aquatic environment? Environ Int 32, 967–976.

[22] Dong, S., Xia, T., Yang, Y., Lin, S., Mao, L., 2018. Bioaccumulation of 14C-labeled graphene in an aquatic food chain through direct uptake or trophic transfer. Environ Sci Technol 52, 541–549.

[23] Arvidsson, R., Molander, S., Sandén, B.A., 2013. Review of potential environmental and health risks of the nanomaterial graphene. Hum Ecol Risk Assess: Int J 19, 873–887.

[24] Han, Y., Knightes, C.D., Bouchard, D., Zepp, R., Avant, B., Hsieh, H.S., Chang, X., Acrey, B., Henderson, W.M., Spear, J., 2019. Simulating graphene oxide nanomaterial phototransformation and transport in surface water. Environ Sci: Nano 6, 180–194.

[25] Goodwin Jr., G.D., Adeleye, A.S., Sung, L., Ho, K.T., Burgess, R.M., Petersen, E.J., 2018. Detection and quantification of graphene-family nanomaterials in the environment. Environ Sci Technol 52, 4491–4513.

[26] Nouara, A., Wu, Q., Li, Y., Tang, M., Wang, H., Zhao, Y., Wang, D., 2013. Carboxylic acid functionalization prevents the translocation of multi-walled carbon nanotubes at predicted environmentally relevant concentrations into targeted organs of nematode *Caenorhabditis elegans*. Nanoscale 5, 6088–6096.

[27] Katsumiti, A., Cajaraville, M.P., 2019. In vitro testing: in vitro toxicity testing with Bivalve Mollusc and fish cells for the risk assessment of nanoparticles in the

aquatic environment. Ecotoxicology of Nanoparticles in Aquatic Systems. CRC Press, pp. 62–98.

[28] Lammel, T., Boisseaux, P., Fernández-Cruz, M.L., Navas, J.M., 2013. Internalization and cytotoxicity of graphene oxide and carboxyl graphene nanoplatelets in the human hepatocellular carcinoma cell line Hep G2. Part Fibre Toxicol 10 (27).

[29] Katsumiti, A., Tomovska, R., Cajaraville, M., 2017. Intracellular localization and toxicity of graphene oxide and reduced graphene oxide nanoplatelets to mussel hemocytes in vitro. Aquat Toxicol 188, 138–147.

[30] Tu, Y., Lv, M., Xiu, P., Huynh, T., Zhang, M., Castelli, M., Liu, Z., Huang, Q., Fan, C., Fang, H., Zhou, R., 2013. Destructive extraction of phospholipids from Escherichia coli membranes by graphene nanosheets. Nat Nanotechnol 8, 594–601.

[31] Wang, A., Pu, K., Dong, B., Liu, Y., Zhang, L., Zhang, Z., Duan, D., Zhu, Y., 2013. Role of surface charge and oxidative stress in cytotoxicity and genotoxicity of graphene oxide towards human lung fibroblast cells. J Appl Toxicol 33, 1156–1164.

[32] Britto, R.S., Nascimento, J.P., Serodre, T., Santos, A.P., Soares, A.M.V.M., Furtado, C., Ventura-Lima, J., Monserrat, J.M., Freitas, R., 2021. Oxidative stress in *Ruditapes philippinarum* after exposure to different graphene oxide concentrations in the presence and absence of sediment. Comp Biochem Physiol Part C 240, 108922.

[33] Souza, J.P., Baretta, J.F., Santos, F., Paino, I.M.M., Zucolot, V., 2017. Toxicological effects of graphene oxide on adult zebrafish (*Danio rerio*). Aquat Toxicol 186, 11–18.

[34] Khan, B., Adeleye, A.S., Burgess, R.M., Smolowitz, R., Russo, S.M., Ho, K.T., 2019. A 72-h exposure study with eastern oysters (*Crassostrea virginica*) and the nanomaterial graphene oxide. Environ Toxicol Chem 38, 820–830.

[35] Audira, G., Lee, J.S., Siregar, P., Malhotra, N., Rolden, M.J.M., Huang, J.C., Chen, K.H.C., Hsu, H.S., Hsu, Y., Ger, T.R., Hsiao, C.D., 2021. Comparison of the chronic toxicities of graphene and graphene oxide toward adult zebrafish by using biochemical and phenomic approaches. Environ Pollut 278, 116907.

[36] Bortolozzo, L.S., Coa, F., Khan, L.U., Medeiros, A.M.Z., Da Silva, G.H., Delite, F.S., Strauss, M., Martinez, D.T.S., 2021. Mitigation of graphene oxide toxicity in *C. elegans* after chemical degradation with sodium hypochlorite. Chemosphere 278, 130421.

[37] Apul, O.G., Wang, Q., Zhou, Y., Karanfil, T., 2013. Adsorption of aromatic organic contaminants by graphene nanosheets: comparison with carbon nanotubes and activated carbon. Water Res 47, 1648–1654.

[38] He, Y., Liu, Y., Wu, T., Ma, J., Wang, X., Gong, Q., Kong, W., Xing, F., Liu, Y., Gao, J., 2013. An environmentally friendly method for the fabrication of reduced graphene oxide foam with a super oil absorption capacity. J Hazard Mater 260, 796–805.

[39] Ersan, G., Apul, O.G., Perreault, F., Karanfil, T., 2017. Adsorption of organic contaminants by graphene nanosheets: a review. Water Res 126, 385–398.

[40] Wang, J., Zhang, J., Han, L., Wang, J., Zhu, L., Zeng, H., 2021. Graphene-based materials for adsorptive removal of pollutants from water and underlying interaction mechanism. Adv Colloid Interface Sci 289, 102360.

[41] Sanchís, J., Olmos, M., Vincent, P., Farre, M., Barcelo, D., 2016. New insights on the influence of organic co-contaminants on the aquatic toxicology of carbon nanomaterials. Environ Sci Technol 50, 961–969.

[42] Limbach, L.K., Wick, P., Manser, P., Grass, R.N., Bruinink, A., Stark, W.J., 2007. Exposure of engineered nanoparticles to human lung epithelial cells: influence of chemical composition and catalytic activity on oxidative stress. Environ Sci Technol 41, 4158–4163.

[43] Baun, A., Sorensen, S.N., Rasmussen, R.F., Hartmann, N.B., Koch, C.B., 2008. Toxicity and bioaccumulation of xenobiotic organic compounds in the presence of aqueous sus pensions of aggregates of nano-C(60). Aquat Toxicol 86, 379–387.

[44] Hartmann, J., Baun, A., 2010. The nano cocktail: ecotoxicological effects of engineered nanoparticles in chemical mixtures. Integr Environ Assess Manag 6, 311–313.

[45] Canesi, L., Ciacci, C., Balbi, T., 2015. Interactive effects of nanoparticles with other contaminants in aquatic organisms: Friend or foe? Mar Environ Res 111, 128–134.

[46] Deng, R., Lin, D., Zhu, L., Majumdar, S., White, J.C., Gardea-Torresdey, J.L., Xing, B., 2017. Nanoparticle interactions with co-existing contaminants: joint toxicity, bioaccumulation and risk. Nanotoxicology 11, 591–612.

[47] Freixa, A., Acuña, V., Sanchís, J., Farré, M., Barceló, D., Sabater, S., 2018. Ecotoxicological effects of carbon based nanomaterials in aquatic organisms. Sci Total Environ 619–620, 328–337.

[48] Naasz, S., Altenburger, R., Kühnel, D., 2018. Environmental mixtures of nanomaterials and chemicals: the Trojan-horse phenomenon and its relevance for ecotoxicity. Sci Total Environ 635, 1170–1181.

[49] Bhagart, J., Nishimura, N., Shimada, Y., 2021. Toxicological interactions of microplastics/nanoplastics and environmental contaminants: current knowledge and future perspectives. J Hazard Mater 405, 123913.

[50] Hu, J., Zhao, Y., Xu, H., 2022. Trojan horse in the intestine: a review on the biotoxicity of microplastics combined environmental contaminants. J Hazard Mater 439, 129652.

[51] U.E. Water Framework Directive. 2008. Environmental Quality Standards Directive (EQSD). 105/EC. https://ec.europa.eu/environment/water/water-framework/priority_substances.htm.

[52] U. S. EPA, 2014. IRIS Toxicological Review of Benzo[a]pyrene (External Review Draft). U.S. Environmental Protection Agency. EPA/635/R-14/312, Washington, DC.

[53] Banni, M., Sforzini, S., Arlt, V.M., Barranger, A., Dallas, L.J., Oliveri, C., Aminot, Y., Pacchioni, B., Milino, C., Lanfranchi, G., Readman, J.W., 2017. Assessing the impact of benzo[a]pyrene on marine mussels: application of a novel targeted low density microarray complementing classical biomarker responses. PloS One 12, e0178460.

[54] Di, Y., Schroeder, D.C., Highfield, A., Readman, J.W., Jha, A.N., 2011. Tissue-specific expression of p53 and ras genes in response to the environmental genotoxicant benzo(α)pyrene in marine mussels. Environ Sci Technol 45, 8974–8981.

[55] Di, Y., Aminot, Y., Schroeder, D.C., Readman, J.W., Jha, A.N., 2017. Integrated biological responses and tissue-specific expression of p53 and ras genes in marine mussels following exposure to benzo(α)pyrene and C60 fullerenes, either alone or in combination. Mutagenesis 32, 77–90.

[56] Gómez-Mendikute, A., Etxeberria, A., Olabarrieta, I., Cajaraville, M.P., 2002. Oxygen radicals production and actin filament disruption in bivalve haemocytes treated with benzo(a)pyrene. Mar Environ Res 54, 431–436.

[57] Cancio, I., Orbea, A., Völkl, A., Fahimi, H.D., Cajaraville, M.P., 1998. Induction of peroxisomal oxidases in mussels: comparison of effects of lubricant oil and benzo(a)pyrene with two typical peroxisome proliferators on peroxisome structure and function in *Mytilus galloprovincialis*. Toxicol Appl Pharmacol 149, 64–72.

[58] Marigómez, I., Izagirre, U., Lekube, X., 2005. Lysosomal enlargement in digestive cells of mussels exposed to cadmium, benzo[a]pyrene and their combination. Comp Biochem Physiol Part C: Toxicol Pharmacol 141, 188–193.

[59] Tian, S., Pan, L., Sun, X., 2013. An investigation of endocrine disrupting effects and toxic mechanisms modulated by benzo[a]pyrene in female scallop *Chlamys farreri*. Aquat Toxicol 144, 162–171.

[60] González-Soto, N., Hatfield, J., Katsumiti, A., Duroudier, N., Lacave, J.M., Bilbao, E., Orbea, A., Navarro, E., Cajaraville, M.P., 2019. Impacts of dietary exposure to different sized polystyrene microplastics alone and with sorbed benzo[a]pyrene on biomarkers and whole organism responses in mussels Mytilus galloprovincialis. Sci Total Environ 684, 548–566.

[61] Cajaraville, M.P., Pal, S.G., 1995. Morphofunctional study of the haemocytes of the bivalve mollusc *Mytilus galloprovincialis* with emphasis on the endolysosomal compartment. Cell Struct Funct 20, 355–367.

[62] Robledo, C., Marigómez, I., Angulo, E., Cajaraville, M.P., 2006. Glycosylation and sorting pathways of lysosomal enzymes in mussel digestive cells. Cell Tissue Res 324, 319–333.

[63] Martínez-Álvarez, I., Le Menach, K., Devier, M.H., Barbarin, I., Tomovska, R., Cajaraville, M.P., Budzinski, H., Orbea, A., 2021. Uptake and effects of graphene oxide nanomaterials alone and in combination with polycyclic aromatic hydrocarbons in zebrafish. Sci Total Environ 775, 145669.

[64] Katsumiti, A., Nicolussi, G., Bilbao, D., Prieto, A., Etxebarria, N., Cajaraville, M.P., 2019. In vitro toxicity testing in hemocytes of the marine mussel *Mytilus galloprovincialis* (L.) to uncover mechanisms of action of the water accommodated fraction (WAF) of a naphthenic North Sea crude oil without and with dispersant. Sci Total Environ 670, 1084–1094.

[65] UNE-EN 15662:2019. Foods of plant origin - Multimethod for the determination of pesticide residues using GC- and LC-based analysis following acetonitrile extraction/partitioning and clean-up by dispersive SPE - Modular QuEChERS-method https://www.une.org/encuentra-tu-norma/busca-tu-norma/norma?c=N0061576.

[66] UNE-EN ISO/IEC 17025:2017. General requirements for the competence of testing and calibration laboratories (ISO/IEC 17025:2017) https://www.une.org/encuentra-tu-norma/busca-tu-norma/norma/?c=N0059467.

[67] Borenfreund, E., Puerner, J.A., 1985. Toxicity determined in vitro by morphological alterations and neutral red absorption. Toxicol Lett 24, 119–124.

[68] Aebi, H., 1984. Catalase in vitro. Methods Enzymol 105, 121–126.

[69] Bradford, M.M., 1976. A rapid and sensitive method for the quantitation of microgram quantities of protein utilizing the principle of protein-dye binding. Anal Biochem 72, 248–254.

[70] Duroudier, N., Katsumiti, A., Mikolaczyk, M., Schäfer, J., Bilbao, E., Cajaraville, M.P., 2019. Cell and tissue level responses in mussels *Mytilus galloprovincialis* dietarily exposed to PVP/PEI coated Ag nanoparticles at two seasons. Sci Total Environ 750, 141303.

[71] Pinto-Silva, C.R.C., Creppy, E.E., Matias, W.G., 2005. Micronucleus test in mussels *Perna perna* fed with the toxic dinoflagellate *Prorocentrum lima*. Arch Toxicol 79, 422–426.

[72] Bolognesi, C., Fenech, M., 2012. Mussel micronucleus cytome assay. Nat Protoc 7, 1125–1137.

[73] Guilhermino, L., Lopes, M.C., Carvalho, A.P., Soared, A.M.M., 1996. Inhibition of acetylcholinesterase activity as effect criterion in acute tests with juvenile Daphnia magna. Chemosphere 32, 727–738.

[74] Lima, I., Moreira, S.M., Rendón-Von Osten, J., Soares, A.M.M., Guilhermino, L., 2007. Biochemical responses of the marine mussel *Mytilus galloprovincialis* to petrochemical environmental contamination along the North-Western coast of Portugal. Chemosphere 66, 1230–1242.

[75] Ellman, G., Courtney, K., Andres, V., Featherstone, R., 1961. A new and rapid colorimetric determination of acetylcholinesterase activity. Biochem Pharmacol 7, 88–95.

[76] Ellis, G., Goldberg, D.M., 1971. An improved manual and semi-automatic assay for NADP-dependent isocitrate dehydrogenase activity, with a description of some kinetic properties of human liver and serum enzyme. Clin Biochem 2, 175–185.

[77] Habig, W., Pabst, M.J., Jakoby, W.B., 1974. Glutathione S-transferases, the first enzymatic step in mercapturic acid formation. J Biol Chem 249, 7130–7139.

[78] Flohé, L., Günzler, W.A., 1984. Assays of glutathione peroxidase. Methods Enzymol 105, 114–121.

[79] McCord, J., Fridovich, I., 1969. Superoxide dismutase, an enzymic function for erythrocuprein (hemocuprein). J Biol Chem 244, 6049–6055.

[80] Martoja R., Martoja-Pierson M. 1970. Técnicas de Histología Animal. Toray-Masson, Barcelona.

[81] Gamble, M., Wilson, I., 2002. The hematoxylin and eosin. In: Bancroft, J.D., Gamble, M. (Eds.), Theory and Practice of Histological Techniques, 125. Churchill Livingstone-Elsevier Science Ltd., London, IK.

[82] Villalba, A., Mourelle, S.G., Carballal, M.J., Lopez, C., 1997. Symbionts and diseases of farmed mussels *Mytilus galloprovincialis* throughout the culture process in the Rias of Galicia (NW Spain). Dis Aquat Org 31, 127–139.

[83] Garmendia, L., Soto, M., Vicario, U., Kim, Y., Cajaraville, M.P., Marigómez, I., 2011. Application of a battery of biomarkers in mussel digestive gland to assess long term effects of the Prestige oil spill in Galicia and Bay of Biscay: tissue-level biomarkers and histopathology. J Environ Monit 13, 915–932.

[84] Bignell, J., Cajaraville, M.P., Marigómez, I., 2012. Background document: histopathology of mussels (*Mytilus spp.*) for health assessment in biological effects monitoring. Integrated monitoring of chemicals and their effects. In: Davies, I.M., Vethaak, A.D. (Eds.). ICES Cooperative Research Report N. 315, Copenhagen, Denmark, pp. 111–120.

[85] Seed, R., 1969. The ecology of *Mytilus edulis* L (Lamellibranchiata) on exposed rocky shores. Oecologia 3, 277–315.

[86] Kim Y., Ashton-Alcox A., Powell E.N. 2006. Histological techniques for marine bivalve molluscs: update NOAA technical memorandum NOS NCCOS 27, 76 pp.

[87] Ortiz-Zarragoitia, M., Cajaraville, M.P., 2006. Biomarkers of exposure and reproduction-related effects in mussels exposed to endocrine disruptors. Arch Environ Contam Toxicol 50, 361–369.

[88] Navarro, E., Iglesias, J.I.P., Camacho, A.P., Labarta, U., Beiras, R., 1991. The physiological energetics of mussels (*Mytilus galloprovincialis* Lmk) from different cultivation rafts in the Ria de Arosa (Galicia, NW Spain). Aquaculture 94, 197–212.

[89] Ruiz, P., Ortiz-Zarragoitia, M., Orbea, A., Vingen, S., Hjelle, A., Baussant, T., Cajaraville, M.P., 2014. Short- and long-term responses and recovery of mussels *Mytilus edulis* exposed to heavy fuel oil no. 6 and styrene. Ecotoxicology 23, 861–879.

[90] Huang, D., Xu, B., Wu, J., Brookes, P.C., Xu, J., 2019. Adsorption and desorption of phenanthrene by magnetic graphene nanomaterials from water: roles of pH, heavy metal ions and natural organic matter. Chem Eng J 368, 390–399.

[91] Khan, B., Adeleye, A.S., Burgess, R.M., Russo, S.M., Ho, K.T., 2019. Effects of graphene oxide nanomaterial exposures on the marine bivalve, *Crassostrea virginica*. Aquat Toxicol 216, 105297.

[92] Faggio, C., Tsarpali, V., Dailianis, S., 2018. Mussel digestive gland as a model tissue for assessing xenobiotics: an overview. Sci Total Environ 636, 220–229.

[93] Josende, M.E., Nunes, S.M., de Oliveira Lobato, R., González-Durruthy, M., Kist, L.W., Bogo, M.R., Wasielesky, W., Sahoo, S., Nascimento, J.P., Furtado, C.A., Fattorini, D., Regoli, F., Machado, K., Werhli, A.V., Monserrat, J.M., Ventura-Lima, J., 2020. Graphene oxide and GST-omega enzyme: an interaction that affects arsenic metabolism in the shrimp *Litopenaeus vannamei*. Sci Total Environ 716, 136893.

[94] Mesarič, T., Sepčić, K., Drobne, D., Makovec, D., Faimali, M., Morgana, S., Falugi, C., Gambardella, C., 2015. Sperm exposure to carbon-based nanomaterials causes abnormalities in early development of purple sea urchin (*Paracentrotus lividus*). Aquat Toxicol 163, 158–166.

[95] Zhu, S., Luo, F., Chen, W., Zhu, B., Wang, G., 2017. Toxicity evaluation of graphene oxide on cysts and three larval stages of *Artemia salina*. Sci Total Environ 595, 101–109.

[96] Lu, J., Zhu, X., Tian, S., Lv, X., Chen, Z., Jiang, Y., Liao, X., Cai, Z., Chen, B., 2018. Graphene oxide in the marine environment: toxicity to *Artemia salina* with and without the presence of Phe and Cd2+. Chemosphere 211, 390–396.

[97] Souza, J.P., Venturini, F.P., Santos, F., Zucolotto, V., 2018. Chronic toxicity in *Ceriodaphnia dubia* induced by graphene oxide. Chemosphere 190, 218–224.

[98] Zhang, Y., Meng, T., Shi, L., Guo, X., Si, X., Yang, R., Quan, X., 2019. The effects of humic acid on the toxicity of graphene oxide to *Scenedesmus obliquus* and *Daphnia magna*. Sci Total Environ 649, 163–171.

[99] Moore, M.N., Viarengo, A.G., Somerfield, P.J., Sforzini, S., 2013. In: Amiard-Triquet, C., Amiard, J.C., Rainbow, P.S. (Eds.), Linking lysosomal biomarkers and ecotoxicological effects at higher biological levels. Ecological Biomarkers: Indicators of Ecotoxicological Effects. CRC Press, Boca Raton (Florida), New York & Oxford, pp. 107–130.

[100] Moore, M.N., Sforzini, S., Viarengo, A., Barranger, A., Aminot, Y., Readman, J.W., Khlobystov, A.N., Arlt, V.M., Banni, M., Jha, A.N., 2021. Antagonistic cytoprotective effects of C60 fullerene nanoparticles in simultaneous exposure to benzo[a]pyrene in a molluscan animal model. Sci Total Environ 755, 142355.

[101] Ren, C., Hu, X., Li, X., Zhou, Q., 2016. Ultra-trace graphene oxide in a water environment triggers Parkinson's disease-like symptoms and metabolic disturbance in zebrafish larvae. Biomaterials 93, 83–94.

[102] Chatterjee, N., Kim, Y., Yang, J., Roca, C.P., Joo, S.W., Choi, J., 2017. A system toxicology approach reveals the Wnt-MAPK crosstalk pathway mediated reproductive failure in *Caenorhabditis elegans* exposed to graphene oxide (GO) but not to reduced graphene oxide (rGO). Nanotoxicology 11, 1.

[103] Dziewięcka, M., Karpeta-Kaczmarek, J., Augustyniak, M., Rost-Roszkowska, M., 2017. Short-term in vivo exposure to graphene oxide can cause damage to the gut and testis. J Hazard Mater 328, 80–89.

[104] Dziewięcka, M., Witas, P., Karpeta-Kaczmarek, J., Kwaśniewska, J., Flasz, B., Balin, K., Augustyniak, M., 2018. Reduced fecundity and cellular changes in

Acheta domesticus after multigenerational exposure to graphene oxide nanoparticles in food. Sci Total Environ 635, 947–955.

[105] Flasz, B., Dziewiecka M.,Kedziorski, A., Tarnawska, M., Augustynjiak, M., 2020. Vitellogein expression, DNA damage, health status of cells and catalase activity in *Acheta domesticus* selected according to their longevity after graphene oxide treatment. Sci Total Environ 737, 140274.

[106] Zhao, S., Wang, Y., Duo, L., 2021. Biochemical toxicity, lysosomal membrane stability and DNA damage induced by graphene oxide in earthworms. Environ Pollut 269, 116225.

[107] Meng, X., Li, F., Wang, X., Liu, J., Ji, C., Wu, H., 2020. Toxicological effects of graphene on mussel *Mytilus galloprovincialis* hemocytes after individual and combined exposure with triphenyl phosphate. Mar Pollut Bull 151, 110838.

[108] Lalwani, G., D'Agati, M., Khan, A.M., Sitharaman, B., 2016. Toxicology of graphene-based nanomaterials. Adv Drug Deliv Rev 105, 109–144.

[109] Cajaraville, M.P., Hauser, L., Carvalho, G., Hylland, K., Olabarrieta, I., Lawrence, A.J., Lowe, D., Goksoyr, A., 2003. Chapter 2: Links between genetic damage by xenobiotics at the individual level and the molecular /cellular response to pollution. In: Lawrence, A.J., Hemingway, K.L. (Eds.), Effects of Pollution on Fish: Molecular Effects and Population Responses. Blackwell Science Ltd, Oxford, pp. 14–82.

[110] Viarengo, A., Lowe, D., Bolognesi, C., Fabbri, E., Koehler, A., 2007. The use of biomarkers in biomonitoring: a 2-tier approach assessing the level of pollutant-induced stress syndrome in sentinel organisms. Comp Biochem Physiol Part C: Toxicol Pharmacol 146, 281–300.

[111] Barranger, A., Langan, L.M., Sharma, V., Rance, G.A., Aminot, Y., Weston, N.J., Akcha, F., Moore, M.N., Arlt, V.M., Khlobystov, A.N., Readman, J.W., Jha, A.N., 2019. Antagonistic interactions between benzo[a]pyrene and fullerene (C60) in toxicological response of marine mussels. Nanomaterials 9, 87.

[112] Barranger, A., Rance, G.A., Aminot, Y., Dallas, L.J., Sforzini, S., Weston, N.J., Lodge, R.W., Banni, M., Arlt, V.M., Moore, M.N., Readman, J.W., Viarengo, A., Khlobystov, A.N., Jha, A.N., 2019. An integrated approach to determine interactive genotoxic and global gene expression effects of multiwalled carbon nanotubes (MWCNTs) and benzo[a]pyrene (BaP) on marine mussels: evidence of reverse 'Trojan Horse' effects. Nanotoxicology 1, 1324–1343.

[113] Chen, S., Qu, M., Ding, J., Zhang, Y., Wang, Y., Di, Y., 2018. BaP-metals co-exposure induced tissue-specific antioxidant defense in marine mussels *Mytilus coruscus*. Chemosphere 205, 286–296.

[114] Coppola, F., Bessa, A., Henriques, B., Russo, T., Soares, A.V.M., Figueira, E., Marques, P.A.P., Polese, G., Di Cosmo, A., Pereira, E., Freitas, R., 2020. Oxidative stress, metabolic and histopathological alterations in mussels exposed to remediated seawater by GO-PEI after contamination with mercury. Comp Biochem Physiol -Part A: Mol Integr Physiol 243, 110674.

[115] Coppola, F., Jiang, W., Soares, A.V.M., Marques, P.A.P., Polese, G., Pereira, M.E., Jiang, Z., Freitas, R., 2021. How efficient is graphene-based nanocomposite to adsorb Hg from seawater. A laboratory assay to assess the toxicological impacts induced by remediated water towards marine bivalves. Chemosphere 277, 130160.

[116] Meng, X., Li, F., Wang, X., Liu, J., Ji, C., Wu, H., 2019. Combinatorial immune and stress response, cytoskeleton and signal transduction effects of graphene and triphenyl phosphate (TPP) in mussel *Mytilus galloprovincialis*. J Hazard Mater 378, 120778.

[117] Bi, C., Junaid, M., Liu, Y., Guo, W., Jiang, X., Pan, B., Li, Z., Xu, N., 2022. Graphene oxide chronic exposure enhanced perfluorooctane sulfonate mediated toxicity through oxidative stress generation in freshwater clam *Corbicula fluminea*. Chemosphere 297, 134242.

[118] Chen, G.Y., Yang, H.J., Lu, C.H., Chao, Y.C., Hwang, S.M., Chen, C.L., Lo, K.W., Sung, L.Y., Luo, W.Y., Tuan, H.Y., Hu, Y.C., 2012. Simultaneous induction of autophagy and toll-like receptor signaling pathways by graphene oxide. Biomaterials 33, 6559–6569.

[119] Chen, Z., Yu, C., Khan, I.A., Tang, Y., Liu, S., Yang, M., 2020. Toxic effects of different-sized graphene oxide particles on zebrafish embryonic development. Ecotoxicol Environ Saf 197, 110608.

[120] Aarab, N., Minier, C., Lemaire, S., Unruh, E., Hansen, P.D., Larsen, B.K., Andersen, O.K., Narbonne, J.F., 2004. Biochemical and histological responses in mussel (*Mytilus edulis*) exposed to North Sea oil and a mixture of North Sea oil and alkylphenols. Mar Environ Res 58, 437–441.

[121] Baussant, T., Ortiz-Zarragoitia, M., Cajaraville, M.P., Bechmann, R.K., Taban, I.C., Sanni, S., 2011. Effects of chronic exposure to dispersed oil on selected reproductive processes in adult blue mussels (*Mytilus edulis*) and the consequences for the early life stages of their larvae. Mar Pollut Bull 62, 1437–1445.

[122] Jing-jing, M., Lu-qing, P., Jing, L., Lin, Z., 2009. Effects of benzo[a]pyrene on DNA damage and histological alterations in gonad of scallop *Chlamys farreri*. Mar Environ Res 67, 47–52.

[123] Yang, Y., Zhou, Y., Pan, L., Xu, R., Li, D., 2020. Benzo[a]pyrene exposure induced reproductive endocrine-disrupting effects via the steroidogenic pathway and estrogen signaling pathway in female scallop *Chlamys farreri*. Sci Total Environ 726, 138585.

[124] Yang, Y., Pan, L., Zhou, Y., Xu, R., Miao, J., Gao, Z., Li, D., 2021. Damages to biological macromolecules in gonadal subcellular fractions of scallop *Chlamys farreri* following benzo[a]pyrene exposure: contribution to inhibiting gonadal development and reducing fertility. Environ Pollut 283, 117084.

[125] Banni, M., Negri, A., Dagnino, A., Jebali, J., Ameur, S., Boussetta, H., 2010. Acute effects of benzo[a]pyrene on digestive gland enzymatic biomarkers and DNA damage on mussel *Mytilus galloprovincialis*. Ecotoxicol Environ Saf 73, 842–848.

[126] Kamel, N., Attig, H., Dagnino, A., Boussetta, H., Banni, M., 2012. Increased temperatures affect oxidative stress markers and detoxification response to benzo

[a]pyrene exposure in mussel *Mytilus galloprovincialis*. Arch Environ Contam Toxicol 63, 534–543.

[127] Guo, B., Feng, D., Xu, Z., Qi, P., Yan, X., 2021. Axute benzo[a]pyrene exposure induced oxidative stress, neurotxocity and epigenetic change in blood clam *Tegillarca granosa*. Sci Rep 11, 18744.

[128] Hu, X., Wei, Z., Mu, L., 2017. Graphene oxide nanosheets at trace concentrations elicit neurotoxicity in the offsprung of zebrafish. Carbon 117, 182–191.

[129] Urban-Malinga, B., Jakubowska, M., Hallmann, A., Dabrowska, A., 2021. Do the graphene nanoflakes pose a potential threat to the polychaete *Hediste diversicolor?* Chemosphere 269, 128685.

[130] Ding, J., Chen, S., Qu, M., Wang, Y., Di, Y., 2020. Trophic transfer affects cytogenetic and antioxidant responses of the mussel *Mytilus galloprovincialis* to copper and benzo(α)pyrene. Mar Environ Res 154, 104848.

[131] Cheung, C.C.C., Siu, W.H.L., Richardson, B.J., Luca-Abbott, S.B.D., Lam, P.K.S., 2004. Antioxidant responses to benzo[a]pyrene and Aroclor 1254 exposure in the greenlipped mussel, *Perna viridis*. Environ Pollut 128, 393–403.

[132] Wang, C., Zhao, Y., Zheng, R., Ding, X., Wei, W., Zuo, Z., Chen, Y., 2006. Effects of tributyltin, benzo[a]pyrene, and their mixture on antioxidant defense systems in *Sebastiscus marmoratus*. Ecotoxicol Environ Saf 65, 381–387.